Outage Probability analysis for an IRS-Assisted System with and without Source-Destination Link for the Case of Quantized Phase Shifts

A Project Report

submitted by

MAVILLA CHARISHMA (EE19M020)

in partial fulfilment of requirements
for the award of the degree of

MASTER OF TECHNOLOGY

Department of ELECTRICAL ENGINEERING
INDIAN INSTITUTE OF TECHNOLOGY MADRAS

June 2021

CERTIFICATE

This is to certify that the thesis titled **Outage Probability analysis for an IRS-Assisted System with and without Source-Destination Link for the Case of Quantized Phase Shifts**, submitted by MAVILLA CHARISHMA (EE19M020), to the Indian Institute of Technology Madras, for the award of the degree of **MASTER OF TECHNOLOGY** is a bona fide record of the work done by her under my supervision. The contents of this report, in full or in parts, have not been submitted to any other Institute or University for the award of any degree or diploma.

Dr. SHEETAL KALYANI
Project Guide
Assistant Professor
Department of Electrical Engineering
IIT Madras, 600 036.

Place: Chennai

Date: 10.06.2021

ACKNOWLEDGEMENTS

I am greatly indebted to **Dr. Sheetal Kalyani** mam for guiding me through the entire course of my M.Tech. project. I would like to thank **Dr. Sheetal Kalyani** mam for giving me valuable suggestions, motivation and insights throughout the project. She always took the time and effort to discuss the problem and to suggest different methods to experiment. Her valuable remarks always gave new directions to my project.

I am thankful to all the professors whose courses helped me improve my knowledge in Wireless Communication and Signal Processing through the course of the two years of my M.Tech. program. Their classes always inspired me to think beyond classrooms into more practical scenarios.

A special thanks to **Athira Subhash** and **Shashank Shekhar** who were my fellow bandits in doing this project. This project would not have been possible without their contributions and insighful observations. A special word of thanks to all the wonderful people I met at IIT Madras without whom life would not have been the same.

ABSTRACT

In this work, we study the outage probability (OP) at the destination of an intelligent reflecting surface (IRS) assisted communication system in the presence of phase error due to quantization at the IRS when a) source-destination (SD) link is present and b) SD link is absent. First, an exact expression is derived and then we derive two simple approximations for the OP using the following approaches: (i) moment matching and, (ii) Kullback–Leibler divergence minimization. The resulting expressions for OP are simple to evaluate and quite tight even in the tail region. The validity of these approximations is demonstrated using extensive Monte Carlo simulations. In this work, we also studied the impact of the parameters like the number of bits available for quantization, the position of IRS w.r.t. source and destination and, the number of elements present at IRS on OP. We derived the Upper bounds to OP using Cauchy-Scwartz inequality and upper bound to bessel function of the second kind. We also studied how large an IRS in order to provide reliable communication in the presence of phase error due to quantization at the IRS. We derived the no of reflector elements needed so that OP lie within an threshold and also optimized the OP for an IRS given an upper bound on the IRS elements.

KEYWORDS: Intelligent reflecting surface, phase error, outage probability, Kullback–Leibler divergence.

TABLE OF CONTENTS

LIST OF TABLES

LIST OF FIGURES

ABBREVIATIONS

IRS	Intelligent Reflecting Surface
OP	Outage Probability
SNR	Signal to noise ratio
SD link	Source to Destination link
CDF	Cumulative distribution function
PDF	Probability distribution function
SISO	Single Input Single Output
KL divergence	Kullback–Leibler divergence
RV	Random Variable

NOTATION

S	Source
D	Destination
$(\cdot)^T$	transpose of a vector
$[\cdot]_i$	i-th element of a vector
β	path loss factor
θ_i	phase shift of the i_{th} IRS element
Θ_i	phase error of the i_{th} IRS element
d_{ab}	distance between nodes **a** and **b**
$\mathbb{P}[A]$	probability of the event A
$\mathbb{E}[X]$	expectation of the RV X
$\mathcal{CN}(0, \sigma^2)$	Complex Gaussian random variable with mean zero and variance σ^2
$\text{diag}(a_1, \cdots, a_N)$	diagonal matrix with entries $a_1, \cdots, a_N$
arg(z)	argument (phase) of the complex number z.

CHAPTER 1

INTRODUCTION

Will 5G technology be just an evolution of 4G technology, or will these emerging technologies needs rethinking of cell centric structure? What are the technologies that will define 5G?

1.1 Need for New Technologies

It's time to look for new multi-antenna technologies to meet the requirements of higher data rate, reliability, and traffic demands in the era of beyond 5G. Two such methods are adaptive beamforming gains and spatial multiplexing which leads to high data. Sine, access to wireless connectivity becomes essential, our requirements of coverage and service quality is growing continously. Present Architecture needs major redesign. At a system level, the frame-based approaches which is heart of 4G need rethinking to meet the requirements for latency and flexible allocation of resources to a massive number of devices as mentioned below:

- Existing coding methods rely on long code words which are applicable to only very short data blocks.
- Short data blocks also worse the efficiencies connected with control and channel estimation overheads. At present, the control plane is robust but sub optimal since it represents fraction of payload data which needs an optimized design.

There is an improvement in terms of latency, data traffic, but only achieved by Users near to cell centers, while the inter-cell interference and handover issues limist the performance of users at cell-edge. To address these, beyond-5G networks needs cell-free structure, where the absence of cell boundaries alleviates the inter-cell interference and handover issues but can also lands up with new challenges.

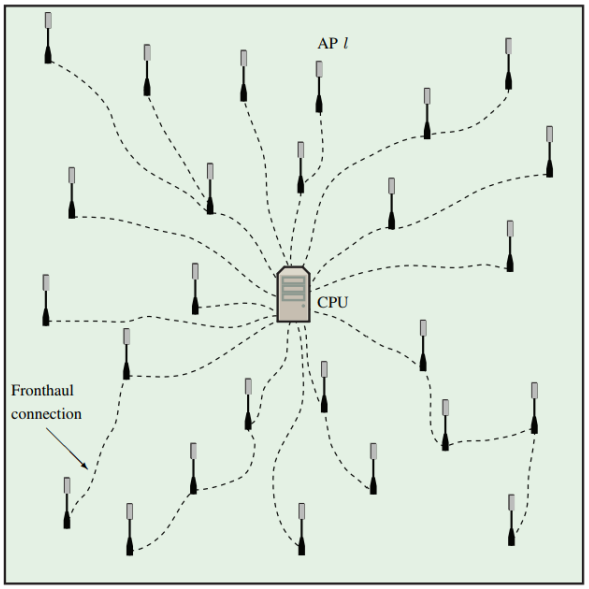

Figure 1.1: Network architecture of Cell Free massive MIMO [1]

1.2 Emerging Technologies

1.2.1 Cell free Massive-MIMO

Communicating with user far away needs very high power. So, we now send data to nearby AP which sends data to the user can be done with relativley low power. But, densification of AP's can increase inter-cell interference and handovers must be frequent. These days the traffic is mostly at cell edges and hence its better to connect with aset of AP's, However, this needs fronthaul signaling for CSI, data sharing and huge complexity. To reduce the fronthaul signaling and computational complexity, a common approach was to divide the network into disjoint clusters with few neighboring AP's. This network-centric approach can provide performance gains, but cannot addresses the interference and handover issues. The resolve these issues, each user is served by those AP's that can reach with non-negligible interference which makes an user-centric network, where each AP collaborates with different sets of AP's when serving different Users.[**?**]

A cell-free massive MIMO network consists of a large number of AP's serving a very smaller number of UE's on the same time-frequency resource. The network operates in TDD mode and exploits UL-DL channel reciprocity, so that each

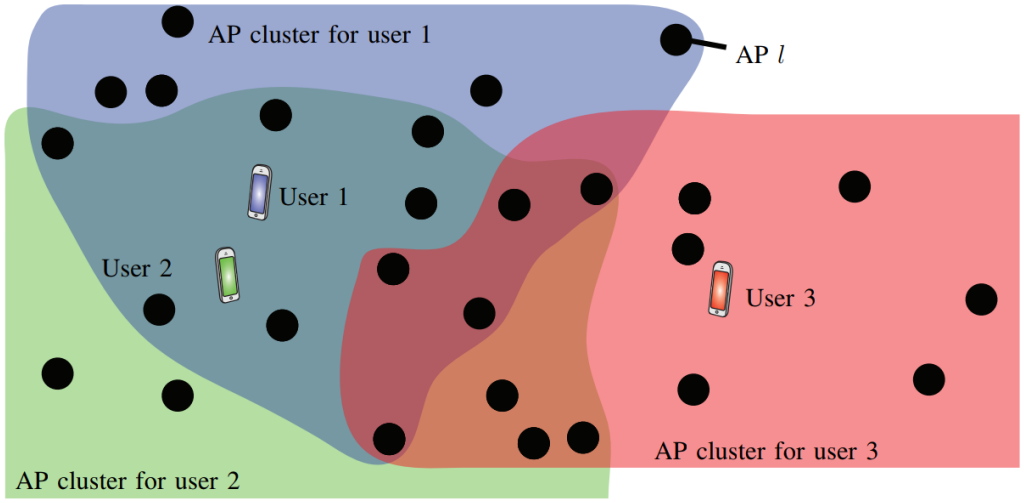

Figure 1.2: Overlapping sets of AP's serving each User [1]

AP can acquire CSI between itself and all UEs from uplink pilots. This CSI is sufficient to implement coherent transmission and reception, so only data signals must be shared between AP's. To enable such information flows, the AP's are assumed to be connected via fronthaul to cloud-edge processors that take care of data encoding and decoding. Fig. 1.1 shows the basic network architecture of a cell-free massive MIMO system and Fig. 1.2 shows how the AP's can be divided into partially overlapping subsets when serving the Users[1].

1.2.2 Beam space massive MIMO

Implementation of MIMO becomes difficult when carrier frequency and bandwidth are increased. We can reduce difficulty level by using spatial structure of the channels and transceiver hardware. The simplest kind of SISO adaptation is linear precoding, where a multiple antenna signal multiplied with precoding matrix is adapted to spatial CSI. With small array sizes, direct digital processing of precoding was practical because it is cost-effective for small arrays to use a relatively high-resolution analog-to-digital converter (ADC) at each transmit element. As we are incrementing the number of antenna's, we need to change the signal processing and implementation of linear precoding.

1.2.3 Millimetre-wave communication

While spectrum is scarce at microwave frequencies, it is plentiful in the mmWave range of frequencies. MmWave cellular research must consider effects of blockages and need for higher density infrastructure and relays. Adaptive arrays decreases interference,so that we can operate in noise-limited conditions. mmWave systems requires large power mainly to ADC's and DAC's. Thus, all antennas cannot be connected to ADC/DAC due to power limitations unless there is an advancement in semiconductor technology. One alternative is a hybrid architecture where beamforming is performed in analog at RF, and multiple sets of beamformers are connected to a small number of ADCs or DACS; where we require signal processing algorithms for assigning weights. Another alternative is to connect each RF chain to a 1-bit ADC/DAC, with very low power requirements; in this case, the beamforming would be performed digitally but on very noisy data. There are abundant research challenges in optimizing different transceiver strategies, analyzing their capacity, incorporating multiuser capabilities, and leveraging channel features such as sparsity. mmWave requires radical changes in the system, as it has a strong impact in both the component and architecture designs.

1.2.4 Device to device (D2D) communication

In voice-centric systems, distance between the callers will be large. But now, its quite different, we use to stay in close proximity when sharing the data (e.g., pictures sharing, video gaming or social networking) wirelessly. Handling these communication scenarios via simply connecting through the network involves gross inefficiencies at various levels:

- Multiple wireless hops are required. This entails a multifold waste of signaling resources as well as higher latency.
- Transmit powers of a fraction of a Watt (in the uplink) and several Watts (in the downlink) are required. This, in turn, entails unnecessary levels of battery drain and interference to all other devices occupying the same signaling resources elsewhere.
- Given that the path losses to possibly distant base stations are much stronger than direct link ones, the corresponding spectral efficiencies are also lower.

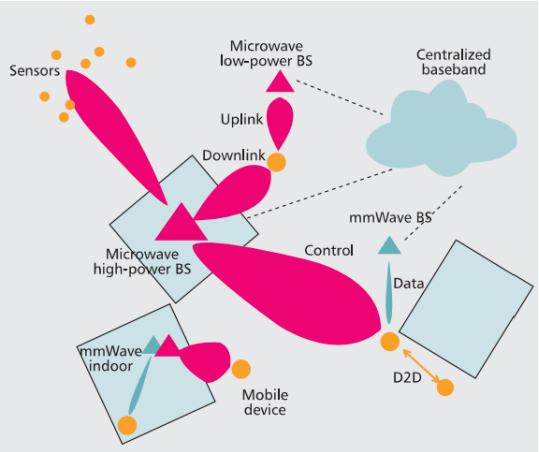

Figure 1.3: Network architecture of D2D communication [2]

While it is clear that D2D will be very much better with Bluetooth or WiFi direct. Mixture of low-latency and high-data-rate constraints (e.g., interaction between users via augmented reality) were main reasons for the use of D2D. Fig. 1.3 shows an example network architecture of D2D communication system [2].

1.3 Existed Comparision of IRS with conventional methods

Unlike cell-free massive MIMO systems and cooperative relays, which also attempt to improve the propagation conditions by deploying active hardware components, an IRS is believed to only require a small operational power making it suitable for implementation in energy-limited systems. Besides, an IRS can operate naturally in a full-duplex manner without the need of costly self-interference cancelation. Furthermore, IRS is made of thin material, allowing for nearly invisible deployment on building facades and interior walls. Hence, once a conventional network has been deployed, one or multiple IRSs can be flexibly deployed to mitigate coverage holes that have been detected or to provide additional capacity in areas where that is needed. In fact, the IRS is not supposed to replace or compete with conventional massive MIMO, MM-wave, NOMA, backscatter communication but rather complement it.

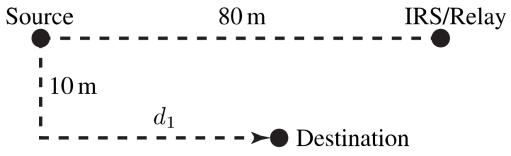

(a) Simulation set up [3]

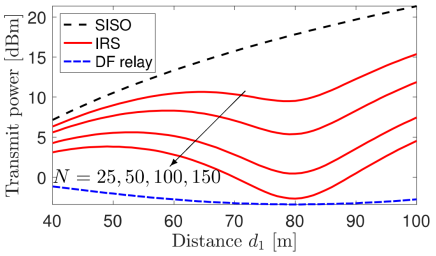

(b) comparision of transmit power with DF relay at rate 6 bits/Hz [3]

1.3.1 Decode and forward Relay

IRS needs hundreds of reconfigurable elements to compete with DF Relay in terms of Rate[3]. The reason is that the source's transmit power must travel over two channels to reach the destination, leading to a very small channel gain $h^{SR}h^{RD}$ per element in the IRS. Hence, the IRS needs many elements to compensate for the low channel gain. In contrast, with DF relaying, we first transmit over a channel with gain h^{SR} and then transmit again over a channel with gain h^{RD}. IRS requires no power amplifiers in its ideal form. An IRS achieves higher Energy efficiency than DF relaying [3]. The fact that the source and destination are physically separated from the IRS is the key feature—it allows for controlling the propagation environment—but also the reason for the large path losses. Classical reflect arrays are using nearby sources equipped with high-gain horn antennas to manage the path loss. In general, it is the total size of the IRS that determines the pathloss. IRS with hundreds of elements needed to beat DF relaying, can be still physically rather small since each element is assumed to have a sub-wavelength size. Simulation set-up for comparision is shown in Figure 1.4a. From figure 1.4b, we can observe that large N can beat DF relay and thus can be claimed as energy efficient system.

1.3.2 Amplify and forward Relay

Fig. 1.5 shows that the IRS provides higher security outcomes than DF Relay and AF Relay varying the distance between the Eavesdropper and the IRS/relay with different powers 10db and 20db, and the scales parameters of the Gamma-

distributed channel of each hop.

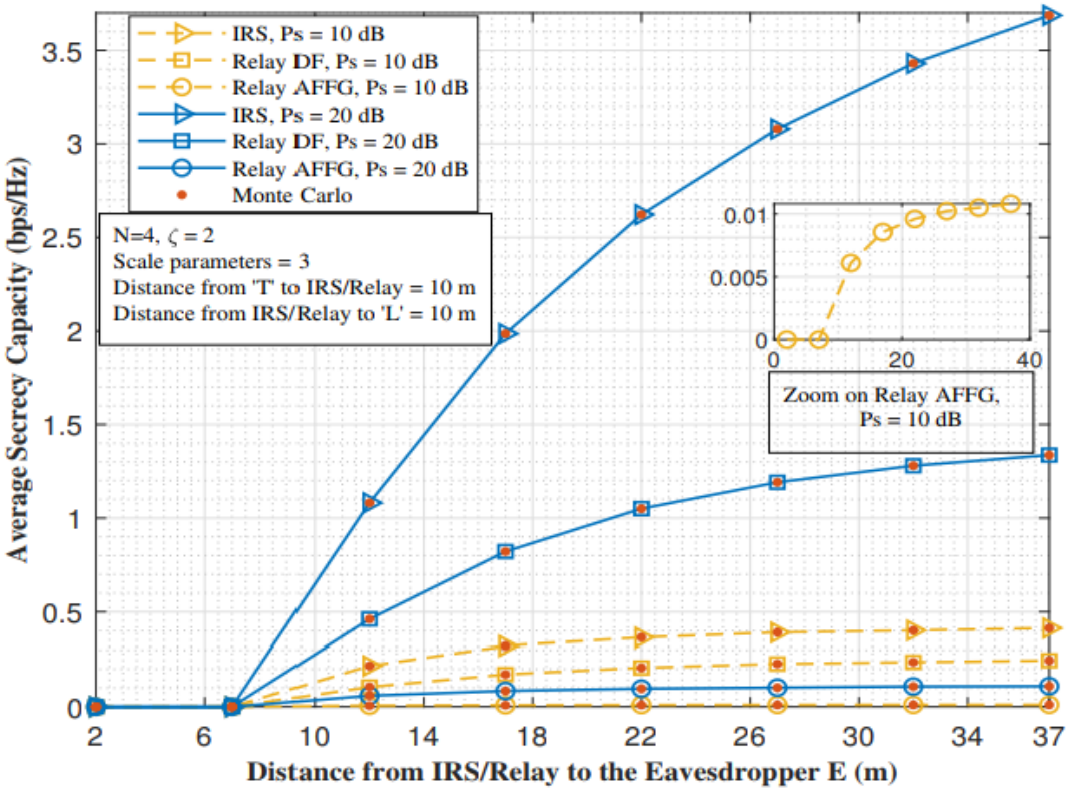

Figure 1.5: comparision of Ergodic capacity with AF Relay [4]

1.4 Literature Survey

Intelligent reflecting surface (IRS) assisted communication has gained much research momentum recently [7]. Reconfigurable IRS's realized using arrays of passive antenna elements or scattering elements made from metamaterials can introduce specific phase shifts on the incident electromagnetic signal without any decoding, encoding, or radiofrequency processing operations [8]. Traditionally, reliable communication links were achieved by implementing intelligent transmitter and receiver designs that combat signal deteriorations introduced by the propagation environment. However, in the past few years, there has been a shift in this paradigm towards the idea of smart radio environments (SRE) where the performance gains achievable via 'smartly' modifying the wireless propagation channel

are explored [7]. Several multiple antenna technologies (Cell-free massive MIMO, beamspace MIMO, and IRS) improving capacity and reliability attracted research momentum towards beyond-5G[1].

Several works in literature study the performance of SRE realized using IRS and compare them with the performance achievable using techniques like cooperative relaying, massive multiple-input multiple-output (M-MIMO), distributed antennas, backscatter communication, millimeter (mm)-wave communication, and network densification [9, 10, 11, 12, 13]. The authors of [10] show that an IRS-assisted M-MIMO system can use the same channel estimation overhead as an M-MIMO system with no IRS to achieve a higher user signal to interference and noise ratio (SINR). The authors of [14] study the performance gains achieved by an IRS-assisted M-MIMO system integrated with a non-orthogonal multiple access (NOMA) network. They also discuss the critical challenges in realizing an IRS-aided NOMA network. The key differences and similarities between an IRS-aided network and a relay network are studied by the authors of [9]. Using mathematical analysis and numerical simulations, they demonstrate that a sufficiently large IRS can outperform relay-aided systems in terms of data rate while reducing the implementation complexity. The number of reflector elements required to outperform the performance of the decode and forward (DF) relay system is studied by the authors of [3]. IRS-aided bistatic backscatter communication (BackCom) system is studied in [11]. Notably, the joint optimization of the phase shifts at the IRS and the transmit beamforming vector of the carrier emitter that minimizes the transmit power consumption is studied. Another exciting venue where IRS has useful applications are the mm-wave communication systems [12, 15, 13]. Authors of [12] proposed three different low-cost architectures based on IRS for beam index modulation scheme in mm-wave communication systems. These schemes are capable of eliminating the line-of-sight blockage of millimeter wave frequencies. The authors of [15] modelled the small scale fading in mm-wave communication by fluctuating two-ray (FTR) distribution and studied the OP and average bit error rate from statistical characterization of SNR of both IRS aided and Amplify and forward(AF) systems. They also showed the superiority of IRS aided system over AF system in mm-wave communication even with small number reflecting

elements. The authors of [13] also study the prospects of combating issues in mm-wave systems like severe path loss and blockage using an IRS to provide effective reflected paths and hence enhance the coverage.

The works discussed above consider performance metrics such as the outage probability (OP), rate and spectral efficiency to evaluate the performance of the IRS-aided communication network. Several works in literature propose different approximations for the OP of an IRS aided system involving one source and one destination node. The authors of [16] assume the availability of a large number of reflector elements and hence use the central limiting theorem (CLT) to derive an approximate expression for the OP. Similarly, the authors of [17] also derive an approximation for the OP using CLT. Unlike the system model in [16], they assume that the direct link between the source and the destination is in a permanent outage. Such Gaussian approximations are also used to characterize metrics like ergodic capacity, secrecy outage probability in many other works including [18, 19, 20, 21]. Similarly, Gamma approximations (using moment matching) are used for deriving approximate OP by the authors of [22, 23, 24, 25]. As mentioned by the authors of [25], the Gamma distribution is a Type-III Pearson distribution and is widely used in fitting distributions for positive random variables (RVs) [26, 27]. The authors of [18, 21, 28, 23] consider more practical IRS models, where due to hardware constraints the possible phase shifts at the IRS elements are restricted to a finite set of discrete values. Table 1.1 provides a brief summary of the critical literature on this topic[1]. Here, the antenna model refers to the antenna model of the source and destination pair devices. From the table, it is apparent that the study of OP considering both b bit phase quantization at the IRS and an active source-destination (SD) link is not available in the open literature.

In this work, we present an exact expression and two different simple approximations for characterizing the OP at the destination of an IRS-assisted communication network. Here, we consider a practical scenario where the phase shift at the IRS elements only takes a finite number of possible values owing to the quan-

[1]Note that the authors of [25] also use Gamma approximation. However, they consider a different path loss model for a system without an SD link and hence, neither we include [25] in Table 1.1 nor we compare our performance with their results.

Reference	Kind of approximation	Impairment	Antenna model	SD link
[16],[29]	CLT and hence gaussian approximation	No	SISO	[16]:Yes [29]: No
[22],[24]	Gamma moment mathching for sum of double Rayleigh	No	SISO	[24]:Yes [22]: No
[30],[23]	Gamma approximation [30]:for double-rayleigh, [23]: for SNR	Yes, quantisation error for [30]: 1 bit phase [23]: b bit phase	SISO	[30]:Yes [23]: No
This work	(a) Approximation for exact integral for outage (b) Gamma Moment matching (c) Gamma KL divergence min	Yes, quantisation error for b bit phase representation	SISO	Yes

Table 1.1: Key literature studying the OP of IRS-assisted communication systems.

tization of the phase values at the IRS. Furthermore, we evaluate the system's performance both in the presence and absence of a direct link between the source and the destination node. Our major contributions are summarised as follows:

- We derive an exact expression for the OP in terms of a multi-fold integral.
- Using the method of moment matching[2], we approximate the received SNR in an IRS-assisted communication system as a Gamma RV and hence derive a simple expression for the corresponding OP.
- We also derive the parameters of the Gamma distribution that has the least Kullback–Leibler (KL) divergence with the exact distribution of SNR[3]. We thus characterize the OP in terms of the CDF of the resulting Gamma RV.
- We also observed the impact of parameters like the number of bits available for quantization, the position of IRS w.r.t.source and destination and, the number of elements present at IRS on OP for an IRS systems with and without an SD link.

[2]The authors of [23] and [22] also uses moment matching to obtain a Gamma approximation, however in scenarios without an SD link and without quantization error respectively. Our approximation for the received SNR is for a more general scenario and it recovers the result in [23] as a special case.

[3]The Gamma distribution, which has minimum KL divergence with respect to the distribution of the received SNR cannot be obtained by moment matching.

- We derived the bounds to OP using cauchy-Scwartz inequality and upper bound to bessel function of second kind.
- We derive the optimal number of reflector elements for the OP to lie within a threshold.
- We also derive the minimum OP obtained for a given number of IRS elements.

1.5 Organization

The rest of the paper is organized as follows. The system model we consider is presented in Chapter 2. Next, in Chapter 3, we propose two methods to evaluate the OP and later we proposed a closed form expression for OP for generalized fading model and hence can obtain OP for all fading environments. In Chapter4, we have presented the bounds on OP using Cauchy-Scwartz inequality and Bessel upper bound. In Next Chapter 5, we have formulated a problem statement to find how large an IRS should be for an OP to fall below a threshold. We also studied what could be the minimum possible OP for a given number of IRS reflector elements. In chapter 6, we verify the utility of our expressions through simulation experiments and present insights regarding the impact of various system parameters on the OP and finally, Chapter 7 concludes the work.

CHAPTER 2

SYSTEM MODEL

2.1 Intelligent Reflecting Surface

Electromagnetic waves undergo multiple uncontrollable alterations as they propagate with in a wireless environment. Free space path loss, signal absorption, as well as reflections, refractions, and diffractions caused by physical objects within the environment highly affect the performance of wireless communications. IRS concept builds on manipulating the propagation of EM waves in channel so as to improve the performance of communication systems. Specifically, IRS is a planar surface comprising a large number of low-cost passive reflecting elements, each being able to induce an amplitude and/or phase change to the incident signal independently, thereby collaboratively achieving fine-grained three-dimensional (3D) reflect beamforming [3].

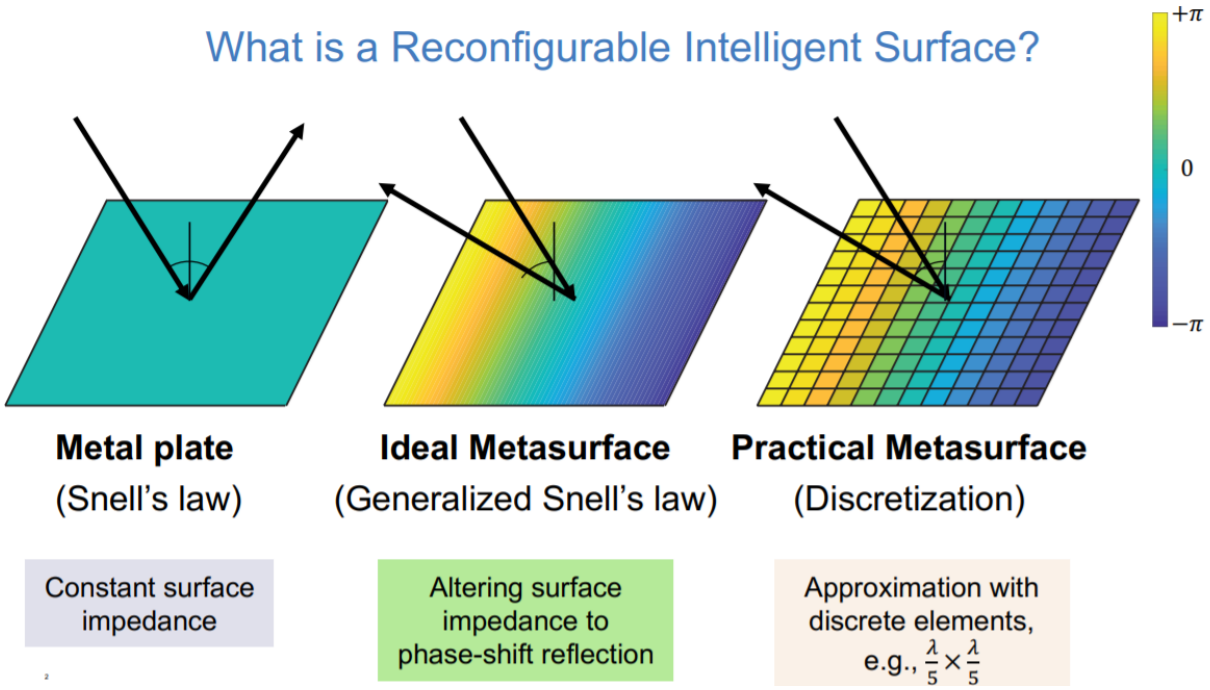

Figure 2.1: Concept of Meta Surface [5]

Figure 2.1 explains basic idea of IRS surface i.e forming a meta surface with discretized impedences to favour beam forming towards user. Normally, a flat finite-sized surface reflects the incoming wave in the main direction determined by Snell's law but with a beamwidth that is inversely proportional to the size of the surface relative to the wavelength. The use of metasurfaces cannot change the reflection losses, but it can create anomalous reflections, meaning that the main direction of the reflected signal can be controlled. This can be achieved by letting every point on the surface induce a certain phase shift to the incoming signal. Ideally, this should be done in a continuous way over the surface, but metasurfaces approximate this using many discrete "meta-atoms" of a sub-wavelength size that each induces a distinct phase-shift. Hence, an IRS is an array of meta-atoms that each scatter the incoming signals with a controllable phase-shift, so that the joint effect of all phase-shifts is a reflected beam in a selected direction.

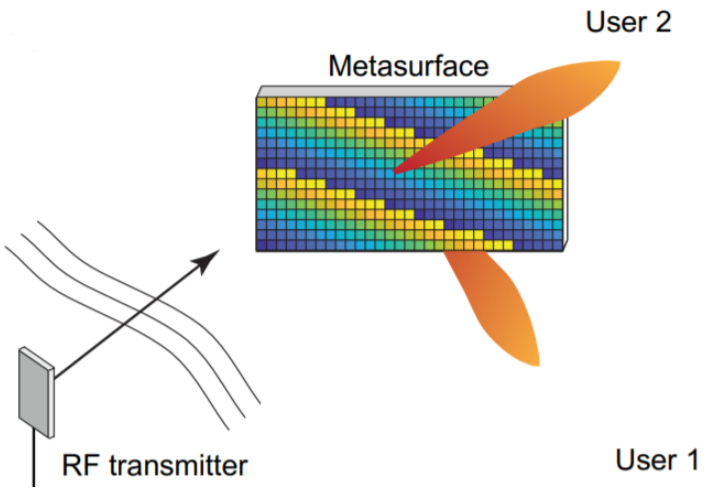

Figure 2.2: beam forming [6]

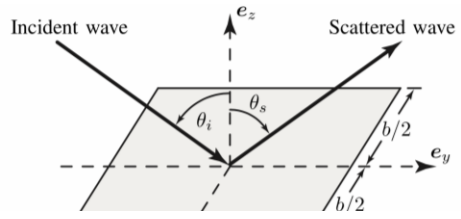

Figure 2.3: Model for Fig. 2.4 [6]

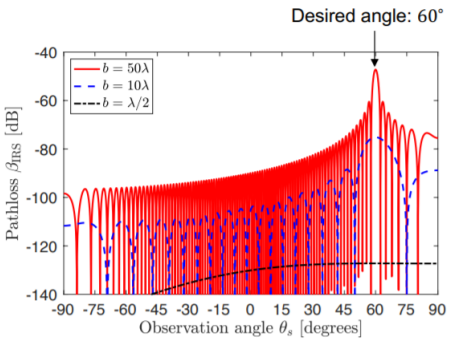

Figure 2.4: Pathloss for different sizes of IRS elements [6]

Fig. 2.3 shows the relation between incident signal and scattered signal for different values of IRS size. There is a trade off between beam width and size of reflector plate, if desired beam width is small then IRS has to be large. Fig. 2.2 illustrates how different phase-shift patterns among the meta-atoms lead to the incoming signal being reflected as a beam in different directions. IRS proactively modifies the wireless channel between them via highly controllable and intelligent signal reflection. This thus provides a new degree of freedom (DoF) to further enhance the wireless communication performance and paves the way to realize a smart and programmable wireless environment. Since IRS eliminates the use of transmit RF chains and operates only in short range, it can be densely deployed with scalable cost and low energy consumption, yet without the need of sophisticated interference management among passive IRSs.

2.1.1 Architecture

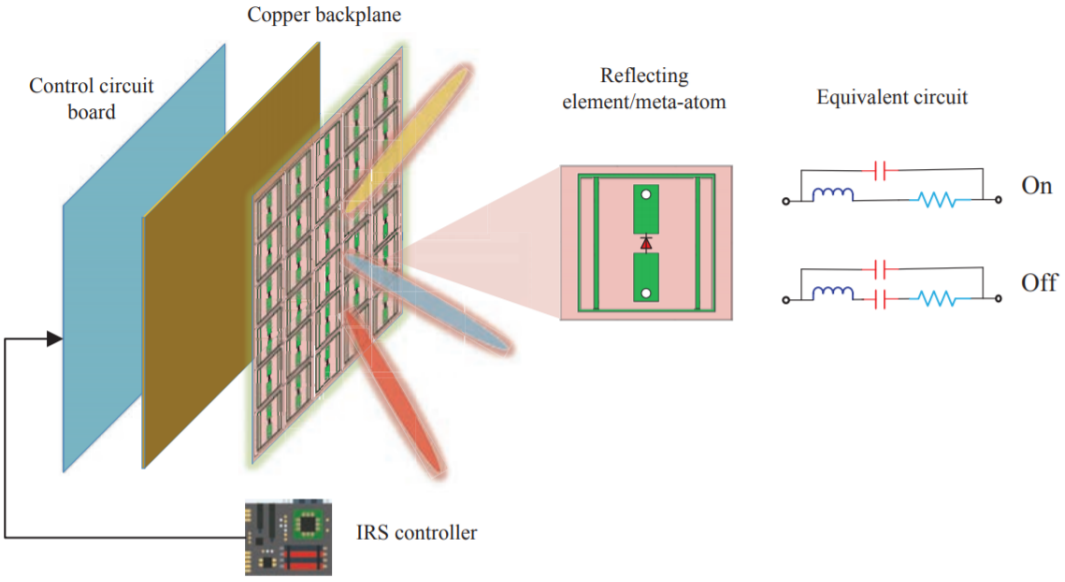

Figure 2.5: Hardware Architecture [5]

Fig 2.5 shows the basic architecture of IRS equipped with meta atoms whose shape , size, orientation, arrangement etc controls individual signal response (reflection amplitude and phase shift). We can also observe that there were three layers and a smart controller. In the outer layer, a large number of metallic elements are printed on a dielectric substrate to directly interact with incident signals. Behind

this layer, a copper plate aids from signal energy leakage. Last, the inner layer is a control circuit board adjusts amplitude/phase shift of each element, triggered by a smart controller attached to the IRS.

PIN diode is embedded in each element which is switched between "ON" and "OFF" bycontrolling its biasing voltage via a direct-current feeding line which generates a phase-shift difference of π in radians. Thus phase shifts of all the elements are controlled by adjusting biasing voltage with the help of smart controller. On the other hand, to effectively control the reflection amplitude i.e by changing the values of resistors in each element, different portions of the incident signal's energy are dissipated, thus achieving controllable reflection amplitude in the range [0, 1]. In practice, it is desirable to have independent control of the amplitude and phase shift at each element for which those two needs to be integrated.

2.1.2 Applications

In this sub-section, we illustrates several typical applications of IRS. IRS coherently combines the individually scattered signals, thereby creating a signal beam focused at the user i.e energy focusing. Fig. 2.6, illustrates several applications of IRS-aided wireless networks[5]. First application shows that User at dead zone can receive significant power when bypassed the signal through IRS. Second apllication shows that IRS can be employed to nullify the signal at eavesdropper (energy nulling). Third application exemplifies how an user at cell edge can nullify the signal from nearby Base station and receives desired signal. Fourth application n illustrates the use of IRS for enabling massive device-to-device connectivity. The last application exemplifies the use of IRS for realizing simultaneous wireless information and power transfer to various devices in an Internet-of-Things network.

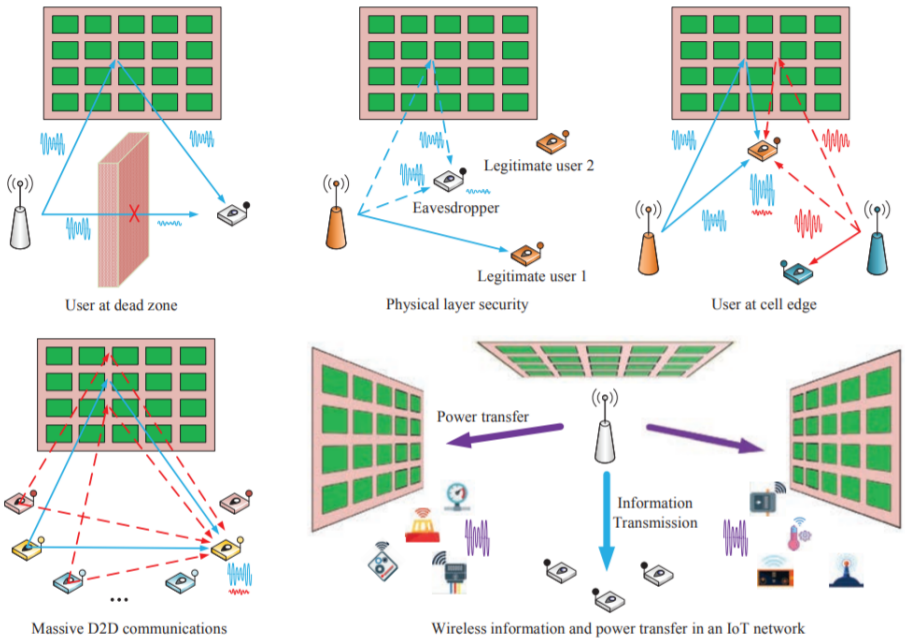

Figure 2.6: Applications of IRS [5]

2.2 System model

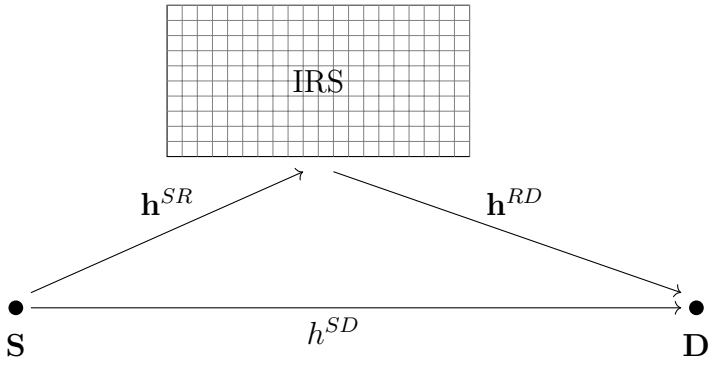

Figure 2.7: System Model

We consider a system consisting of one source node (**S**) communicating with one destination node (**D**) using an **IRS** with N reflector elements as shown in Fig. 2.7. Here **S** and **D** are both equipped with a single antenna each. Furthermore, we assume that the distance between **IRS** and **S**/**D** is large enough such that all elements of the **IRS** are at the same distance from **S**/**D**. Let, $\mathbf{h}^{SR} \in \mathbb{C}^{N\times 1}$, $\mathbf{h}^{RD} \in \mathbb{C}^{N\times 1}$ and $h^{SD} \in \mathbb{C}^{1}$ denote the small-scale fading channel coefficients of the **S** to **IRS**, **IRS** to **D** and **S** to **D** link respectively. It is assumed that all the channels experience independent Rayleigh fading and hence we have, $h^{SD} \sim \mathcal{CN}\left(0, d_{sd}^{-\beta}\right)$,

$\left[\mathbf{h}^{SR}\right]_i \sim \mathcal{CN}\left(0, d_{sr}^{-\beta}\right)$ and $\left[\mathbf{h}^{RD}\right]_i \sim \mathcal{CN}\left(0, d_{rd}^{-\beta}\right)$, $\forall i \in \{1, \cdots, N\}$. Here, β is the path loss coefficient. Let α and θ_i represent amplitude coefficient and phase shift introduced by the i-th **IRS** element, respectively. The signal received at node **D** is then given by,

$$y = \sqrt{p}\left(h^{SD} + \alpha\left(\mathbf{h}^{SR}\right)^T \mathbf{\Theta}\mathbf{h}^{RD}\right)s + n, \tag{2.1}$$

where $\mathbf{\Theta} = \text{ diag}\left(e^{j\theta_1}, ..., e^{j\theta_N}\right)$, p is the transmit power, s is the transmitted signal with $\mathbb{E}[|s|^2]$=1 and n is the AWGN with noise power σ^2. The SNR at the node **D** of the IRS-supported network is then given by

$$\gamma_{IRS} = \gamma_s\left|h^{SD} + \alpha\left(\mathbf{h}^{SR}\right)^T \mathbf{\Theta}\mathbf{h}^{RD}\right|^2, \tag{2.2}$$

where $\gamma_s = \frac{p}{\sigma^2}$. To achieve maximum SNR at **D**, the phase-shift of the i-th IRS element needs to be selected as follows [21],

$$\theta_i^{opt} = \arg\left(h^{SD}\right) - \arg\left(\left[\mathbf{h}^{SR}\right]_i\left[\mathbf{h}^{RD}\right]_i\right). \tag{2.3}$$

Let b be the number of bits used to represent the phase. Then the set of all possible phase shifts at each of the IRS element is given by $\{0, \frac{2\pi}{2^b}, \cdots, \frac{(2^b-1)2\pi}{2^b}\}$ [21]. Hence, θ_i^{opt} may not be always available and the exact phases shift at the i-th IRS element can be represented as $\theta_i = \theta_i^{opt} + \Phi_i$, where Φ_i denotes the phase error at the i^{th} reflector. Note that, $-2^{-b}\pi \leq \Phi_i \leq 2^{-b}\pi$ and we model $\Phi_i \sim \mathcal{U}[-2^{-b}\pi, 2^{-b}\pi]$ [31], [21]. Here, $\mathcal{U}[a, b]$ represents the uniform distribution over the support $[a, b]$. Thus, the expression for SNR incorporating the phase error term is given as follows:

$$\gamma_{IRS} = \gamma_s\left(\left|\left|h^{SD}\right| + \alpha\sum_{i=1}^{N}\left|\left[\mathbf{h}^{SR}\right]_i\right|\left|\left[\mathbf{h}^{RD}\right]_i\right|e^{j\Phi_i}\right|^2\right). \tag{2.4}$$

Note that, our system model and channel model are identical to [21]. In the next section, we use (2.4) to derive an exact expression and then simple approximations for the OP at **D**.

CHAPTER 3

OUTAGE PROBABILITY

3.1 Outage probability

Outage at a node is the phenomenon of the instantaneous SNR falling below a particular threshold, say γ. The OP at node **D** can be evaluated as,

$$P_{outage} = \mathbb{P}\left[\gamma_{IRS} < \gamma\right]. \tag{3.1}$$

Note that γ_{IRS} is the square of the absolute value of the sum of a Rayleigh RV and a sum of i.i.d. double Rayleigh RVs [32] each scaled by the exponential of a uniform RV. The PDF of a double Rayleigh RV can be expressed in terms of the modified Bessel function [32, (1)]. Hence the distribution of the sum of N such scaled double Rayleigh RVs has a very complicated expression[30, 22]. This makes the characterization of the exact distribution of the OP a mathematically intractable task. So far, there were various kinds of approximations for OP (as shown in Table 1.1) proposed in the open literature. However, to the best of our knowledge, none of them considered the most general case, *i.e.*, the presence of an SD link and b-bit quantization error. Hence, in the subsequent subsections, we consider the most general case and present an exact expression and three different simple approximations for (3.1).

3.1.1 Exact Outage Expresion

In this subsection, we first derive an exact expression for the CDF of SNR, in the form of a multi-fold integration where the order of integration grows linearly with the number of elements in the IRS. Solving this multi-fold integration analytically is mathematically intractable and we demonstrate how the method of moment matching can circumvent this issue. [33] can be used to circumvent this issue.

Lemma 1. *For a threshold γ, an exact expression for OP at node* **D** *is given by*

$$P_{outage} = \left(\frac{2^{b+1} d_{sr}^{\beta} d_{rd}^{\beta}}{\pi \gamma_s}\right)^N \int \cdots \int \left[\left(1 - e^{\frac{-\left(\sqrt{\gamma - (\mathbf{s}^T\mathbf{x})^2} - \mathbf{c}^T\mathbf{x}\right)^2 d_{sd}^{\beta}}{\gamma_s}}\right) \mathrm{U}\left(\sqrt{\gamma - (\mathbf{s}^T\mathbf{x})^2} - \mathbf{c}^T\mathbf{x}\right) \prod_{i=1}^{N} x_i K_0 \left[\frac{2x_i}{\sqrt{\gamma_s} d_{sr}^{-\beta/2} d_{rd}^{-\beta/2}}\right] \right] dx_1 d\phi_1 \ldots dx_N d\phi_N, \tag{3.2}$$

where $\mathbf{c} = [\alpha\cos(\phi_1)\ldots\alpha\cos(\phi_N)]^T$, $\mathbf{s} = [\alpha\sin(\phi_1)\ldots\alpha\sin(\phi_N)]^T$, $\mathbf{x} = [x_1, \ldots, x_N]$, K_0 *is modified Bessel function of the second kind of order zero [34] and* $\mathrm{U}(\cdot)$ *is the unit step function.*

Proof. Please refer Appendix A.1 for the proof. □

Note that (3.2) provides an exact expression for the OP at **D**, but it is a multi-fold integration of order $2N$. It is very difficult to evaluate this expression even numerically for values of N such as 50 using common mathematical softwares such as Matlab/Mathematica. So, it is important to have an approximation that is close to (3.2) and also easily computable. One such approximation is obtained by Gamma moment matching.

3.1.2 Gamma approximation using Moment matching

In this sub-section, we approximate the SNR as a Gamma RV with shape parameter k_{mom} and scale parameter θ_{mom} by matching their first and second moments. Using this result, the OP at node **D** is given by the following theorem.

Theorem 1. *The OP for a threshold γ at node* **D** *can be evaluated as*

$$P_{outage} = \frac{\gamma^{k_{mom}}}{\theta_{mom}^{k_{mom}} \Gamma\left(k_{mom}+1\right)} {}_1F_1\left(k_{mom}, k_{mom}+1, \frac{-\gamma}{\theta_{mom}}\right), \tag{3.3}$$

where the shape parameter (k_{mom}) and the scale parameter (θ_{mom}) of the Gamma distribution can be evaluated using:

$$\theta_{mom} = \frac{\mathbb{E}[\gamma_{IRS}^2] - \mathbb{E}^2[\gamma_{IRS}]}{E[\gamma_{IRS}]}, \tag{3.4}$$

$$k_{mom} = \frac{\mathbb{E}[\gamma_{IRS}]}{\theta_{mom}}. \tag{3.5}$$

Here, ${}_1F_1(\cdot,\cdot,\cdot)$ *is the confluent hypergeometric function of the first kind [35] and* $\mathbb{E}[\gamma_{IRS}], \mathbb{E}[\gamma_{IRS}^2]$ *can be evaluated using (A.28) and (A.29) respectively.*

Proof. Please refer Appendix A.2 for the proof. □

Note that the expression in (3.3) is very easy to evaluate when compared to the OP approximations proposed in a few of the recent literature including [30, 28, 36]. Also, the proposed approximations hold well both for the cases of small and large values of N, unlike the Gaussian approximations using CLT [20, 25, 19, 18, 29] which holds only for large N. Furthermore, the proposed CDF of γ_{IRS} can be easily used for deriving the expressions of other metrics of interest like the rate [37]. Since we have considered a very general scenario in Theorem 1, we present certain special cases of interest in the following corollaries.

Corollary 1.1. In the absence of phase errors, the OP can be approximated using (3.3), where (3.4) and (3.5) can be evaluated using the following expressions for the moments of SNR.

$$\mathbb{E}[\gamma_{IRS}^{np}] = \gamma_s \left[N\alpha^2 d_{sr}^{-\beta} d_{rd}^{-\beta} + d_{sd}^{-\beta} + N\alpha \frac{\pi^{\frac{3}{2}}}{4} d_{sr}^{\frac{-\beta}{2}} d_{rd}^{\frac{-\beta}{2}} d_{sd}^{\frac{-\beta}{2}} + \alpha^2 \frac{\pi^2 N(N-1)}{16} d_{sr}^{-\beta} d_{rd}^{-\beta} \right]. \tag{3.6}$$

$$\begin{aligned}\mathbb{E}[(\gamma_{IRS}^{np})^2] =& \gamma_s^2 \left[N\alpha^4 d_{sr}^{-2\beta} d_{rd}^{-2\beta} \left[1 + 3N + \frac{3\pi^2(N-1)(2N-1)}{16} + \frac{(N-1)(N-2)(N-3)\pi^4}{256} \right] \right. \\ &+ 2d_{sd}^{-2\beta} + 3N\alpha^2 d_{sr}^{-\beta} d_{rd}^{-\beta} d_{sd}^{-\beta} \left[2 + \frac{(N-1)\pi^2}{8} \right] + \frac{3N\alpha\pi^{3/2}}{4} d_{sd}^{-\frac{3\beta}{2}} d_{sr}^{-\frac{\beta}{2}} d_{rd}^{-\frac{\beta}{2}} \\ &\left. + N\alpha^3 \pi^{\frac{3}{2}} d_{sd}^{-\frac{\beta}{2}} d_{sr}^{-\frac{3\beta}{2}} d_{rd}^{-\frac{3\beta}{2}} \left[\frac{\pi^2(N-1)(N-2)}{32} + \frac{3(4N-1)}{8} \right] \right]. \end{aligned} \tag{3.7}$$

Proof. Equations (5.17) and (5.18) are obtained from (A.28) and (A.29) by substituting $b \to \infty$. □

Corollary 1.2. When the SD link is in a permanent outage, the OP can be approximated using (3.3) where equations (3.4) and (3.5) can be evaluated using

the following equations:

$$\mathbb{E}[\gamma_{IRS}^{ndl}] = \gamma_s N\alpha^2 d_{sr}^{-\beta} d_{rd}^{-\beta}\left[1 + \frac{\pi^2}{8}\frac{(N-1)}{2}s^2\right]. \tag{3.8}$$

$$\begin{aligned}\mathbb{E}[\left(\gamma_{IRS}^{ndl}\right)^2] =& \gamma_s^2 N\alpha^4 d_{sr}^{-2\beta} d_{rd}^{-2\beta}\left[2 + 2N + (N-1)p^2 + \frac{(N-1)(4N+1)}{16}\pi^2 s^2\right.\\ &\left. + \frac{(N-1)(N-2)(N-3)}{256}\pi^4 s^4 + \frac{(N-1)(N-2)\pi^2 s^2 p}{8}\right],\end{aligned} \tag{3.9}$$

where $s = \frac{2^b}{\pi}\sin\left(\frac{\pi}{2^b}\right), p = \frac{2^b}{2\pi}\sin\left(\frac{2\pi}{2^b}\right)$.

Proof. When the SD link is in a permanent outage, the phase error at the i-th reflector element is given by $\Phi_i := \theta_i - \theta_{opt}$ where $\theta_{opt} = -\arg\left([\mathbf{h}_{sr}]_i [\mathbf{h}_{rd}]_i\right)$. Here also, we model the phase error as a uniform RV, *i.e.*, $\Phi_i \sim \mathcal{U}\left[-2^{-b}\pi, 2^{-b}\pi\right]$. In this case, the SNR expression given in equation (2.4) can be modified as follows:

$$\gamma_{IRS}^{ndl} = \gamma_s\left|\alpha\sum_{i=1}^{N}\left|\left[\mathbf{h}^{SR}\right]_i\right|\left|\left[\mathbf{h}^{RD}\right]_i\right|e^{j\Phi_i}\right|^2. \tag{3.10}$$

Next, we follow the steps similar to Appendix A.2 and arrive at (5.24) and (5.25). □

Note that Corollary 1.2 recover existing results presented in [23, (9)] and [23, (10)] respectively.

Corollary 1.3. In the absence of phase errors and when the SD link is in a permanent outage, the OP can be approximated using (3.3) where equations (3.4) and (3.5) can be evaluated using following equations:

$$\mathbb{E}[\gamma_{IRS}^{npdl}] = \gamma_s\left[N\alpha^2 d_{sr}^{-\beta} d_{rd}^{-\beta} + \alpha^2\frac{\pi^2 N(N-1)}{16}d_{sr}^{-\beta} d_{rd}^{-\beta}\right]. \tag{3.11}$$

$$\mathbb{E}[(\gamma_{IRS}^{npdl})^2] = \frac{N\alpha^4\gamma_s^2}{d_{sr}^{2\beta} d_{rd}^{2\beta}}\left[1 + 3N + \frac{3\pi^2(N-1)(2N-1)}{16} + \frac{(N-1)(N-2)(N-3)\pi^4}{256}\right]. \tag{3.12}$$

Proof. Equations (5.30) and (5.31) are obtained from (5.24) and (5.25) by substi-

tuting $s, p \to 1$. □

Note that Corollary 1.3 recover existing results presented in [23, (14)] and [23, (15)], respectively.

The gamma approximation based on moment matching is simple and could be applied to all considered scenarios but was not tight. Hence, we tried to improve upon it by looking for that gamma approximation which has the minimum KL divergence with respect to the actual SNR.

3.1.3 KL divergence minimization

In this section, we identify the parameters of a Gamma distribution such that the KL divergence between the resulting RV and the exact SNR is the least among all possible Gamma distributions. Using this result, the OP at **D** is given by the following theorem:

Theorem 2. *The OP for a threshold γ at the node* **D** *is given by*

$$P_{outage} = \frac{\gamma^{k_{kl}}}{\theta_{kl}^{k_{kl}} \Gamma\left(k_{kl}+1\right)} {}_1F_1\left(k_{kl}, k_{kl}+1, \frac{-\gamma}{\theta_{kl}}\right), \tag{3.13}$$

where k_{kl} and θ_{kl} are obtained by solving the following two equations:

$$\mathbb{E}[\log(\gamma_{IRS})] = \log(\theta_{kl}) + \psi(k_{kl}), \tag{3.14}$$

$$\mathbb{E}[\gamma_{IRS}] = k_{kl} \times \theta_{kl}. \tag{3.15}$$

Here, ${}_1F_1(.,.,)$ is the confluent hypergeometric function of the first kind [35] and $\psi(.)$ is the digamma function [38].

Proof. Please refer Appendix A.3 for the proof. □

The derivation of the exact expression for evaluating $\mathbb{E}[\log(\gamma_{IRS})]$ is complicated and hence we proceed with the following approximation for the same [37, (11)]:

$$\mathbb{E}[\log \gamma_{IRS}] \approx \log\left(\mathbb{E}[\gamma_{IRS}]\right) - \frac{1}{2}\frac{\mathbb{E}[\gamma_{IRS}^2] - \mathbb{E}^2[\gamma_{IRS}]}{\mathbb{E}^2[\gamma_{IRS}]}. \tag{3.16}$$

Given that we can compute the first and second moments of γ_{IRS} using (A.28) and (A.29), we can easily evaluate (3.16). Then we can solve for the parameters k_{kl} and θ_{kl} using the solvers available in any mathematical software such as *Matlab, Mathematica, or Octave*. Thus, the method of KL divergence minimization also provides us with a simple expression for the OP that is very amenable for computation and further analysis.

Corollary 2.1. For the special cases without SD link or phase error or both, the OP for a threshold γ is given by (3.13). Corresponding values of scale and shape parameters can be solved using equations (3.14) and (3.15) where the corresponding moments can be evaluated using Corollaries 1.1-1.3.

Note that the approximation for the expectation of the logarithm of SNR provided in (3.16) makes use of only the first and second moment of γ_{IRS} and this approximation does not hold equally well throughout the support of γ_{IRS}. This was particularly observed in the simulations of certain special cases like scenarios without the SD link. Hence, we propose the following method to circumvent this issue for scenarios without an SD link and no phase error. In such a case we have,

$$\gamma_{IRS}^{npdl} = \gamma_s \left(\alpha \sum_{i=1}^{N} \left| \left[\mathbf{h}^{SR}\right]_i \right| \left| \left[\mathbf{h}^{RD}\right]_i \right| \right)^2 . \tag{3.17}$$

Now, we can approximate the double Rayleigh RV $[\gamma_{dr}]_i := \left| \left[\mathbf{h}^{SR}\right]_i \right| \left| \left[\mathbf{h}^{RD}\right]_i \right|$ as a Gamma RV with shape parameter and scale parameter $k_{kl,dr}$ and $\theta_{kl,dr}$ respectively using the method of KL divergence minimisation[1]. In this case, the expectation of the logarithm of the RV $[\gamma_{dr}]_i$ has a closed-form expression (as given in 3.18) and hence we can avoid the approximation used in (3.16).

$$\mathbb{E}\left[\log\left([\gamma_{dr}]_i\right)\right] = -\psi + \log(d_{sr}^{\frac{-\beta}{2}} d_{sr}^{\frac{-\beta}{2}}) \quad \forall i, \tag{3.18}$$

where ψ is the Euler gamma constant. For the cases with SD link, or $b > 1$, we could not arrive at simple expressions for the distribution of γ_{IRS} even after approximating the double Rayleigh RV as a gamma RV [30].

[1]The authors of [30] also approximates double Rayleigh RVs as a Gamma RV, but using the method of moment matching.

3.1.4 Extension of Gamma approximation for generalized fading

In this sub-section, we find the closed form for OP applicable to all fading environments. Let, $\mathbf{h}^{SR} \in \mathbb{C}^{N\times 1}$, $\mathbf{h}^{RD} \in \mathbb{C}^{N\times 1}$ and $h^{SD} \in \mathbb{C}^{1}$ denote the small-scale fading channel coefficients of the **S** to **IRS**, **IRS** to **D** and **S** to **D** link respectively. It is assumed that all the channels experience any independent fading. We approximate the SNR as a Gamma RV with shape parameter k_{mom} and scale parameter θ_{mom} by matching their first and second moments for generalized fading model. From 1 Using this result, the OP at node **D** is given by the following theorem.

Theorem 3. *The OP for a threshold γ at node* **D** *can be evaluated as*

$$P_{outage} = \frac{\gamma^{k_{mom}}}{\theta_{mom}^{k_{mom}}\Gamma\left(k_{mom}+1\right)} {}_1F_1\left(k_{mom}, k_{mom}+1, \frac{-\gamma}{\theta_{mom}}\right), \tag{3.19}$$

where the shape parameter (k_{mom}) and the scale parameter (θ_{mom}) of the Gamma distribution can be evaluated using:

$$\theta_{mom} = \frac{\mathbb{E}[\gamma_{IRS}^2] - \mathbb{E}^2[\gamma_{IRS}]}{E[\gamma_{IRS}]}, \tag{3.20}$$

$$k_{mom} = \frac{\mathbb{E}[\gamma_{IRS}]}{\theta_{mom}}. \tag{3.21}$$

Here, ${}_1F_1(\cdot,\cdot,\cdot)$ is the confluent hypergeometric function of the first kind [35] and $\mathbb{E}[\gamma_{IRS}], \mathbb{E}[\gamma_{IRS}^2]$ can be evaluated using following equations

$$\mathbb{E}\left[\gamma_{IRS}\right] = \gamma_s\left(m_2^{sd} + N\alpha^2 m_2^{sr} m_2^{rd} + 2Ns\ \alpha m_1^{sd} m_1^{sr} m_1^{rd} + 2\alpha^2 (m_1^{sr})^2 (m_1^{rd})^2 \frac{N(N-1)}{2} s^2\right). \tag{3.22}$$

$$\mathbb{E}\left[{\gamma_{IRS}}^2\right] = \gamma_s^2 \Bigg(m_4^{sd} + 2\alpha^2 N m_2^{sr} m_2^{rd} m_2^{sd} + N\alpha^4 m_4^{sr} m_4^{rd} + 2\alpha^4 \frac{N(N-1)}{2} (m_2^{sr})^2 (m_2^{rd})^2 \tag{3.23}$$

$$+4\alpha^2 m_2^{sd} \left[N m_2^{sr} m_2^{rd} [\frac{1+p}{2}] + 2s^2 \frac{N(N-1)}{2} (m_2^{sr})^2 (m_2^{rd})^2 \right]$$

$$+N(N-1)\alpha^4 \left[(N-2) m_2^{sr} m_2^{rd} s^2 \left(1+p\right) (m_1^{sr})^2 (m_1^{rd})^2 \right.$$

$$\left. +(m_2^{sr})^2 (m_2^{rd})^2 (1+p^2) + s^4 (N-2)(N-3)(m_1^{sr})^4 (m_1^{rd})^4 \right]$$

$$+2 \left[2N\alpha m_3^{sd} m_1^{sr} m_1^{rd} s + 2\alpha^3 N m_1^{sd} m_3^{sr} m_3^{rd} s + 4\alpha^3 m_1^{sd} m_1^{sr} m_1^{rd} m_2^{sr} m_2^{rd} \frac{N(N-1)}{2} s \right]$$

$$+2\frac{N(N-1)}{2} \left[4\alpha^3 m_1^{sd} \left[m_1^{sr}\right]^3 \left[m_1^{rd}\right]^3 (N-2) s^3 + 2 * 4\alpha^3 m_1^{sd} m_2^{sr} m_2^{rd} m_1^{sr} m_1^{rd} s \frac{1+p}{2} \right]$$

$$+4\alpha^2 \frac{N(N-1)}{2} s^2 m_1^{sr} m_1^{rd} \left[m_2^{sd} m_1^{sr} m_1^{rd} + \alpha^2 \left[m_3^{sr} m_3^{rd} + 2 m_1^{sr} m_1^{rd} m_2^{sr} m_2^{rd} (N-2) \right] \right] \Bigg).$$

Proof. Please refer Appendix A.4 for the proof. Here, m_r^{ab} denotes the r^{th} moment of fading distribution, $a, b \in \{\mathbf{S}, \mathbf{R}, \mathbf{D}\}$.

For suppose, let us consider the rician fading model where OP can be found using eqn. 3.19 where the first four moments of rician are given by

$$m_1^{ab} = \sqrt{\frac{\pi}{2}} \sigma_{ab} L_{\frac{1}{2}}(-\frac{v_{ab}^2}{2\sigma_{ab}^2}) \tag{3.24}$$

$$m_2^{ab} = v_{ab}^2 + 2\sigma_{ab}^2 \tag{3.25}$$

$$m_3^{ab} = 3\sqrt{\frac{\pi}{2}} \sigma_{ab}^3 L_{\frac{3}{2}}(-\frac{v_{ab}^2}{2\sigma_{ab}^2}) \tag{3.26}$$

$$m_4^{ab} = v_{ab}^4 + 8 v_{ab}^2 \sigma_{ab}^2 + 8\sigma_{ab}^4 \tag{3.27}$$

Similarly, closed form of an OP can be easily found by substituting their moments in Theorem 3. □

CHAPTER 4

BOUND TO OUTAGE PROBABILITY

4.1 Using Upper bound to Bessel function

In this section, we find the upper bound to OP for an IRS assisted system with and without SD-link assuming perfect channel estimation and also assumed that optimized phase shifts are available. We here use the upper bound to bessel bound given by

$$\mathrm{K}_0(ax) \leq \frac{\sqrt{\pi}e^{-ax}}{\sqrt{2ax}} \tag{4.1}$$

Theorem 4. *The upper bound to OP for a threshold γ at node* **D** *can be evaluated as*

$$\begin{aligned}
P_{outage} \leq & \int_0^{\gamma} \frac{\pi^N a^{\frac{3N}{2}}}{2^{\frac{3N}{2}}} \left[\frac{e^{-at} z^{\frac{3N}{2}-1}}{\Gamma(\frac{3N}{2})}\right] dz \\
& - \frac{\pi^N a^{\frac{3N}{2}}}{2^{\frac{3N}{2}}} \sqrt{\pi} b \int_0^{\gamma} \left[\frac{2^{\frac{3N}{2}-1}(\frac{1}{b^2})^{-\frac{3N}{4}} e^{-\frac{z^2}{4b^2}}}{\Gamma[\frac{3N}{2}] b\sqrt{\Pi}} \left[(\frac{-z}{2b^2}) \left[\Gamma[\frac{3N}{4}] F_1[\frac{3N}{4}, \frac{1}{2}, \frac{(-2ab^2+z)^2}{4b^2}]\right.\right.\right. \\
& \left.\left.\left. + \sqrt{\frac{1}{b^2}}(-2ab^2+z)\Gamma[\frac{1}{2}+\frac{3N}{4}] F_1[\frac{2+3N}{4}, \frac{3}{2}, \frac{(-2ab^2+z)^2}{4b^2}]\right]\right] \\
& + \frac{2^{-1+\frac{3N}{2}}(\frac{1}{b^2})^{-\frac{3N}{4}} e^{-\frac{z^2}{4b^2}}}{\Gamma[\frac{3N}{2}] b\sqrt{\Pi}} \left[\Gamma[\frac{3N}{4}] \frac{3N(-2ab^2+z)}{4b^2} F_1[1+\frac{3N}{4}, \frac{3}{2}, \frac{(-2ab^2+z)^2}{4b^2}]\right. \\
& + \sqrt{\frac{1}{b^2}}\Gamma[\frac{1}{2}+\frac{3N}{4}] F_1[\frac{2+3N}{4}, \frac{3}{2}, \frac{(-2ab^2+z)^2}{4b^2}] \\
& \left. + \sqrt{\frac{1}{b^2}} \frac{(-2ab^2+z)^2}{12b^2} \Gamma[\frac{1}{2}+\frac{3N}{4}] F_1[\frac{6+3N}{4}, \frac{5}{2}, \frac{(-2ab^2+z)^2}{4b^2}]\right] dz,
\end{aligned} \tag{4.2}$$

where $a^2 = \frac{4d_{sr}^{\beta} d_{rd}^{\beta}}{\gamma_s}$, $b^2 = \frac{\gamma_s \sigma_{sd}^2}{2\alpha^2}$, ${}_1F_1(\cdot,\cdot,\cdot)$ *is the confluent hypergeometric function of the first kind [35].*

Proof. Please refer Appendix A.2 for the proof. □

Theorem 5. *When SD-link is in outage, the upper bound to OP for a threshold γ at node* **D** *can be evaluated as*

$$P_{Outage} \leq \frac{\pi^N}{2^{\frac{3N}{2}}} \frac{\gamma(\frac{3N}{2}, a\gamma)}{\Gamma(\frac{3N}{2})} \tag{4.3}$$

Proof. Please refer Appendix A.6 for the proof. □

4.2 Using Cauchy-Scwartz inequality

In this section, we find the lower bound to OP or an IRS assistedsystem with and without SD-link assuming perfect channel estimation and optimized phase shifts are available. We here use Cauchy-Scwartz given by

$$\langle \mathbf{m}_{SR}, \mathbf{m}_{RD} \rangle^2 \leq \langle \mathbf{m}_{SR}, \mathbf{m}_{SR} \rangle . \langle \mathbf{m}_{RD}, \mathbf{m}_{RD} \rangle . \tag{4.4}$$

Theorem 6. *The Lower bound to OP for a threshold γ at node* **D** *can be evaluated as*

$$P_{outage} \geq \int_0^{\gamma} \int_0^{\infty} \int_0^{\frac{y_1}{y_3}} f_{Y_1,Y_2,Y_3}(y_1, y_2, y_3) \; dy_2 \; dy_3 \; dy_1, \tag{4.5}$$

where

$$f_{Y_1,Y_2,Y_3}(y_1, y_2, y_3) = \frac{\frac{1}{2}\left(-y_2 - y_3 + \sqrt{4y_1 + y_2^2 - 2y_2y_3 + y_3^2}\right)}{\sigma_{sd}^2} e^{-\frac{(\frac{1}{2}\left(-y_2-y_3+\sqrt{4y_1+y_2^2-2y_2y_3+y_3^2}\right))^2}{\left(2\sigma_{sd}^2\right)}}$$
$$\frac{1}{\Gamma(N)(2\sigma_{sr}^2)^N} y_2^{N-1} e^{-\frac{y_2}{(2\sigma_{sr}^2)}} \frac{1}{\Gamma(N)(2\sigma_{rd}^2)^N} y_3^{N-1} e^{-\frac{y_3}{(2\sigma_{rd}^2)}} \times \left(4y_1 + (y_2 - y_3)^2\right)^{\frac{-1}{2}}. \tag{4.6}$$

Proof. Please refer Appendix A.7 for the proof. □

Theorem 7. *When SD-link is in outge, the lower bound to OP for a threshold γ*

at node **D** *can be evaluated as*

$$P_{outage} \geq \frac{1}{N^2\Gamma^2[N]}\left(\frac{\gamma}{\gamma_s\sigma_{sr}\sigma_{rd}}\right)^N F\left[\{N,N\},\{1,1+N,1+N\},\frac{\gamma}{\gamma_s\sigma_{sr}\sigma_{rd}}\right] \quad (4.7)$$

$$- NF[\{N\},\{1,1+N\},\frac{\gamma}{\gamma_s\sigma_{sr}\sigma_{rd}}]\left(2\psi + Log[\frac{\gamma}{\gamma_s\sigma_{sr}\sigma_{rd}}]\right) \quad (4.8)$$

$$+ 2N^2\Gamma[N]F_r^{(\{1,0\},\{0,0,0\},\{0\})}\left[\{1,N\},\{1,1,1+N\},\{\frac{\gamma}{\gamma_s\sigma_{sr}\sigma_{rd}}\}\right] \quad (4.9)$$

$$. \quad (4.10)$$

Here, $F(\cdot,\cdot,\cdot)$ $F_r(\cdot,\cdot,\cdot)$ *denotes the generalized and regularized confluent hypergeometric functions [35] and* ψ *is Euler gamma constant.*

Proof. Please refer Appendix A.8 for the proof. □

CHAPTER 5

OPTIMIZATION OF OUTAGE PROBABILITY

In this Chapter, we use the approximated expression of OP at the destination of an IRS-assisted communication network given in 3.1.2. Here, we consider a practical scenario where the phase shift at the IRS elements only takes a finite number of possible values owing to the quantization of the phase values at the IRS. Furthermore, we evaluate the system's performance both in the presence and absence of a direct link between the source and the destination node. Our major contributions are summarised as follows:

- We derive the optimal number of reflector elements for the OP to lie within a threshold.
- We also derive the minimum OP obtained for a given number of IRS elements.

The expression for SNR incorporating the phase error term is given as follows:

$$\gamma_{IRS} = \gamma_s \left(\left| h^{SD} \right| + \alpha \sum_{i=1}^{N} \left| \left[\mathbf{h}^{SR} \right]_i \right| \left| \left[\mathbf{h}^{RD} \right]_i \right| e^{j\Phi_i} \right|^2 \right). \tag{5.1}$$

Let $\nu_0 = \frac{\left| h^{SD} \right|}{\alpha}$, $\nu_i = \left| \left[\mathbf{h}^{SR} \right]_i \right| \left| \left[\mathbf{h}^{RD} \right]_i \right| \; \forall i \in \{1, \cdots, N\}$. Since received power cannot be greater than the transmit power, we have,

$$\frac{p}{\sigma^2} \left(\left| h^{SD} \right| + \alpha \sum_{i=1}^{N} \left| \left[\mathbf{h}^{SR} \right]_i \right| \left| \left[\mathbf{h}^{RD} \right]_i \right| e^{j\Phi_i} \right|^2 \right) \leq \frac{p}{\sigma^2} \left(\left| h^{SD} \right| + \alpha \sum_{i=1}^{N} \left| \left[\mathbf{h}^{SR} \right]_i \right| \left| \left[\mathbf{h}^{RD} \right]_i \right| \right|^2 \right) \leq p \tag{5.2}$$

$$\frac{\alpha^2}{\sigma^2} \left(\left| \nu_0 + \sum_{i=1}^{N} \nu_i \right|^2 \right) \leq 1 \tag{5.3}$$

$$\frac{\alpha^2}{\sigma^2} \left(\sum_{i=0}^{N} \nu_i \right)^2 \leq 1 \tag{5.4}$$

Upper bound on the maximum number of IRS elements can be found from $\Big((N+1)\nu_{max} \Big)^2 \leq \frac{\sigma^2}{\alpha^2}$ and received SNR over the reflection path with the largest gain has

to be greater than 1(i.e $\gamma_s \nu_{max}^2 \geq 1$), receive SNR over the reflection path with the largest gain. On combining both we get $(N+1)^2 \leq \gamma_s \frac{\sigma^2}{\alpha^2}$. Thus, the maximum number of reflector elements is given by $N_{max} \leq \min\{\frac{1}{\nu_{max}}\sqrt{\frac{\sigma^2}{\alpha^2}} - 1, \sqrt{\gamma_s \frac{\sigma^2}{\alpha^2}} - 1\}$.

5.1 Problem Statement

5.1.1 Outage probability Optimization

Outage at a node is the phenomenon of the instantaneous SNR falling below a particular threshold, say γ. The OP at node **D** can be evaluated as,

$$P_{outage}(N) = \mathbb{P}\left[\gamma_{IRS} < \gamma\right]. \tag{5.5}$$

Note that γ_{IRS} is the square of the absolute value of the sum of a Rayleigh RV and a sum of i.i.d. double Rayleigh RVs [32] each scaled by the exponential of a uniform RV. The Outage minimization problem is

$$\min_{\{1 \leq N \leq N_{max}\}} P_{outage}(N) \tag{5.6}$$

Where the OP for a threshold γ at node **D** is given by

$$P_{outage}(N) = \frac{\gamma^{k_{mom}}}{\theta_{mom}^{k_{mom}} \Gamma\left(k_{mom}+1\right)} {}_1F_1\left(k_{mom}, k_{mom}+1, \frac{-\gamma}{\theta_{mom}}\right), \tag{5.7}$$

with the shape parameter (k_{mom}) and the scale parameter (θ_{mom}) of the Gamma distribution evaluated from:

$$\theta_{mom} = \frac{\mathbb{E}[\gamma_{IRS}^2] - \mathbb{E}^2[\gamma_{IRS}]}{E[\gamma_{IRS}]}, \tag{5.8}$$

$$k_{mom} = \frac{\mathbb{E}[\gamma_{IRS}]}{\theta_{mom}}. \tag{5.9}$$

Here, ${}_1F_1(\cdot,\cdot,\cdot)$ is the confluent hypergeometric function of the first kind [35] and

$$\mathbb{E}[\gamma_{IRS}] = \gamma_s[N\alpha^2 d_{sr}^{-\beta} d_{rd}^{-\beta} + d_{sd}^{-\beta} + \alpha\frac{\pi^{\frac{3}{2}}}{4} d_{sr}^{\frac{-\beta}{2}} d_{rd}^{\frac{-\beta}{2}} d_{sd}^{\frac{-\beta}{2}} Ns + \alpha^2\frac{\pi^2}{8} d_{sr}^{-\beta} d_{rd}^{-\beta}\frac{N(N-1)}{2}s^2]. \tag{5.10}$$

$$\begin{aligned}\mathbb{E}\left[\gamma_{IRS}^2\right] = \gamma_s^2 \Bigg[& 2d_{sd}^{-2\beta} + \frac{3Ns\alpha\pi^{3/2}}{4} d_{sd}^{-3\beta/2} d_{sr}^{-\beta/2} d_{rd}^{-\beta/2} + N\alpha^2 d_{sr}^{-\beta} d_{rd}^{-\beta} d_{sd}^{-\beta}\left[\frac{3(N-1)\pi^2 s^2}{8} + 4 + 2p\right] \\ & + N\alpha^4 d_{sr}^{-2\beta} d_{rd}^{-2\beta} 2\left[N+1\right] \\ & + N\alpha^4 d_{sr}^{-2\beta} d_{rd}^{-2\beta}(N-1)\left[p^2 + \frac{(N-2)(N-3)\pi^4 s^4}{256} + \frac{\pi^2 s^2}{16}\left[2p(N-2) + 4N + 1\right]\right] \\ & + N\alpha^3\pi^{3/2} d_{sd}^{-\beta/2} d_{sr}^{-3\beta/2} d_{rd}^{-3\beta/2}\left[(4N+5)\frac{s}{8} + \frac{(N-1)(N-2)\pi^2 s^3}{32} + (N-1)s\left(\frac{1}{2} + \frac{p}{2}\right)\right]\Bigg].\end{aligned} \tag{5.11}$$

where $s = \frac{\sin\left(\frac{\pi}{2^b}\right)}{\frac{\pi}{2^b}}, p = \frac{\sin\left(\frac{2\pi}{2^b}\right)}{\frac{2\pi}{2^b}}$. Note that the value of N from (5.6) is very easy to evaluate when compared to the OP approximations proposed in a few of the recent literature including [30, 28, 36]. Since we have considered a very general scenario, we present certain special cases of interest in the following corollaries.

5.1.1.1 Without phase error

To achieve maximum SNR at **D**, the phase-shift of the i-th IRS element needs to be selected as follows [21],

$$\theta_i^{opt} = \arg\left(h^{SD}\right) - \arg\left(\left[\mathbf{h}^{SR}\right]_i \left[\mathbf{h}^{RD}\right]_i\right). \tag{5.12}$$

With this choice, the received power at destination is given by

$$\gamma_{IRS} = \frac{p}{\sigma^2}\left(\left|h^{SD}\right| + \alpha\sum_{i=1}^{N}\left|\left[\mathbf{h}^{SR}\right]_i\right|\left|\left[\mathbf{h}^{RD}\right]_i\right|\right)^2. \tag{5.13}$$

Let $\nu_0 = \frac{\left|h^{SD}\right|}{\alpha}$, $\nu_i = \left|\left[\mathbf{h}^{SR}\right]_i\right|\left|\left[\mathbf{h}^{RD}\right]_i\right|$ $\forall i \in \{1,\cdots,N\}$. Since received power cannot be greater than the transmit power, we have,

$$\frac{p}{\sigma^2}\left(\left|h^{SD}\right| + \alpha\sum_{i=1}^{N}\left|\left[\mathbf{h}^{SR}\right]_i\right|\left|\left[\mathbf{h}^{RD}\right]_i\right|\right)^2 \leq p \tag{5.14}$$

$$\frac{\alpha^2}{\sigma^2}\left(\left|\nu_0+\sum_{i=1}^{N}\nu_i\right|^2\right) \leq 1 \tag{5.15}$$

$$\frac{\alpha^2}{\sigma^2}\left(\sum_{i=0}^{N}\nu_i\right)^2 \leq 1 \tag{5.16}$$

Upper bound on the maximum number of IRS elements can be found from $\Big((N+1)\nu_{max}\Big)^2 \leq \frac{\sigma^2}{\alpha^2}$ and received SNR over the reflection path with the largest gain has to be greater than 1(i.e $\gamma_s\nu_{max}^2 \geq 1$). On combining both we get $(N+1)^2 \leq \gamma_s\frac{\sigma^2}{\alpha^2}$. Thus, the maximum number of reflector elements is given by $N_{max} \leq \min\{\frac{1}{\nu_{max}}\sqrt{\frac{\sigma^2}{\alpha^2}}-1, \sqrt{\gamma_s\frac{\sigma^2}{\alpha^2}}-1\}$. In the absence of phase errors, we now solve the equation 5.6 using OP approximated from (5.7), where (5.8) and (5.9) can be evaluated using the following expressions for the moments of SNR.

$$\mathbb{E}[\gamma_{IRS}^{np}] = \gamma_s\left[N\alpha^2 d_{sr}^{-\beta}d_{rd}^{-\beta} + d_{sd}^{-\beta} + N\alpha\frac{\pi^{\frac{3}{2}}}{4}d_{sr}^{\frac{-\beta}{2}}d_{rd}^{\frac{-\beta}{2}}d_{sd}^{\frac{-\beta}{2}} + \alpha^2\frac{\pi^2N(N-1)}{16}d_{sr}^{-\beta}d_{rd}^{-\beta}\right]. \tag{5.17}$$

$$\begin{aligned}\mathbb{E}[(\gamma_{IRS}^{np})^2] =& \gamma_s^2\left[N\alpha^4 d_{sr}^{-2\beta}d_{rd}^{-2\beta}\left[1+3N+\frac{3\pi^2(N-1)(2N-1)}{16}+\frac{(N-1)(N-2)(N-3)\pi^4}{256}\right]\right.\\ &+2d_{sd}^{-2\beta}+3N\alpha^2 d_{sr}^{-\beta}d_{rd}^{-\beta}d_{sd}^{-\beta}\left[2+\frac{(N-1)\pi^2}{8}\right]+\frac{3N\alpha\pi^{3/2}}{4}d_{sd}^{-\frac{3\beta}{2}}d_{sr}^{-\frac{\beta}{2}}d_{rd}^{-\frac{\beta}{2}}\\ &\left.+N\alpha^3\pi^{\frac{3}{2}}d_{sd}^{-\frac{\beta}{2}}d_{sr}^{-\frac{3\beta}{2}}d_{rd}^{-\frac{3\beta}{2}}\left[\frac{\pi^2(N-1)(N-2)}{32}+\frac{3(4N-1)}{8}\right]\right].\end{aligned} \tag{5.18}$$

5.1.1.2 Without SD Link

When the SD link is in a permanent outage, the SNR at the node **D** of the IRS-supported network is then given by

$$\gamma_{IRS} = \gamma_s\left|\alpha\left(\mathbf{h}^{SR}\right)^T\Theta\mathbf{h}^{RD}\right|^2, \tag{5.19}$$

where $\gamma_s = \frac{p}{\sigma^2}$. To achieve maximum SNR at **D**, the phase-shift of the i-th IRS element needs to be selected as follows [21],

$$\theta_i^{opt} = -\arg\left(\left[\mathbf{h}^{SR}\right]_i\left[\mathbf{h}^{RD}\right]_i\right). \tag{5.20}$$

Let b be the number of bits used to represent the phase. Then the set of all possible phase shifts at each of the IRS element is given by $\{0, \frac{2\pi}{2^b}, \cdots, \frac{(2^b-1)2\pi}{2^b}\}$ [21]. Hence, θ_i^{opt} may not be always available and the exact phases shift at the i-th IRS element can be represented as $\theta_i = \theta_i^{opt} + \Phi_i$, where Φ_i denotes the phase error at the i^{th} reflector. Note that, $-2^{-b}\pi \leq \Phi_i \leq 2^{-b}\pi$ and we model $\Phi_i \sim \mathcal{U}[-2^{-b}\pi, 2^{-b}\pi]$ [31], [21]. Here, $\mathcal{U}[a, b]$ represents the uniform distribution over the support $[a, b]$. Thus, the expression for SNR incorporating the phase error term is given as follows:

$$\gamma_{IRS} = \frac{p}{\sigma^2}\left(\left|\alpha \sum_{i=1}^{N} \left|\left[\mathbf{h}^{SR}\right]_i\right| \left|\left[\mathbf{h}^{RD}\right]_i\right| e^{j\Phi_i}\right|^2\right). \tag{5.21}$$

Let $\nu_i = \left|\left[\mathbf{h}^{SR}\right]_i\right| \left|\left[\mathbf{h}^{RD}\right]_i\right| \ \forall i \in \{1, \cdots, N\}$. Since received power cannot be greater than the transmit power, we have,

$$\frac{p}{\sigma^2}\left(\left|\alpha \sum_{i=1}^{N} \left|\left[\mathbf{h}^{SR}\right]_i\right| \left|\left[\mathbf{h}^{RD}\right]_i\right| e^{j\Phi_i}\right|^2\right) \leq \frac{p}{\sigma^2}\left(\left|\alpha \sum_{i=1}^{N} \left|\left[\mathbf{h}^{SR}\right]_i\right| \left|\left[\mathbf{h}^{RD}\right]_i\right|\right|^2\right) \leq p \tag{5.22}$$

$$\frac{\alpha^2}{\sigma^2}\left(\sum_{i=1}^{N} \nu_i\right)^2 \leq 1 \tag{5.23}$$

Upper bound on the maximum number of IRS elements can be found from $\left(N\nu_{max}\right)^2 \leq \frac{\sigma^2}{\alpha^2}$ and received SNR over the reflection path with the largest gain has to be greater than 1(i.e $\gamma_s \nu_{max}^2 \geq 1$). On combining both we get $N^2 \leq \gamma_s \frac{\sigma^2}{\alpha^2}$. Thus, the maximum number of reflector elements is given by $N_{max} \leq \min\{\frac{1}{\nu_{max}}\sqrt{\frac{\sigma^2}{\alpha^2}}, \sqrt{\gamma_s \frac{\sigma^2}{\alpha^2}}\}$. we now solve the equation 5.6 using OP approximated from (5.7), where (5.8) and (5.9) can be evaluated using the following equations:

$$\mathbb{E}[\gamma_{IRS}^{ndl}] = \gamma_s N \alpha^2 d_{sr}^{-\beta} d_{rd}^{-\beta}\left[1 + \frac{\pi^2}{8}\frac{(N-1)}{2}s^2\right]. \tag{5.24}$$

$$\begin{aligned}\mathbb{E}[\left(\gamma_{IRS}^{ndl}\right)^2] =& \gamma_s^2 N \alpha^4 d_{sr}^{-2\beta} d_{rd}^{-2\beta}\left[2 + 2N + (N-1)p^2 + \frac{(N-1)(4N+1)}{16}\pi^2 s^2\right. \\ &\left. + \frac{(N-1)(N-2)(N-3)}{256}\pi^4 s^4 + \frac{(N-1)(N-2)\pi^2 s^2 p}{8}\right],\end{aligned} \tag{5.25}$$

where $s = \frac{2^b}{\pi}\sin\left(\frac{\pi}{2^b}\right), p = \frac{2^b}{2\pi}\sin\left(\frac{2\pi}{2^b}\right)$.

5.1.1.3 Without SD Link and without phase error

When the SD link is in a permanent outage, the SNR at the node **D** of the IRS-supported network is then given by

$$\gamma_{IRS} = \gamma_s \left| \alpha \left(\mathbf{h}^{SR} \right)^T \Theta \mathbf{h}^{RD} \right|^2, \tag{5.26}$$

where $\gamma_s = \frac{p}{\sigma^2}$. To achieve maximum SNR at **D**, the phase-shift of the i-th IRS element needs to be selected as follows [21],

$$\theta_i^{opt} = -\arg\left(\left[\mathbf{h}^{SR} \right]_i \left[\mathbf{h}^{RD} \right]_i \right). \tag{5.27}$$

With this choice, the received power at destination is given by

$$\gamma_{IRS} = \frac{p}{\sigma^2} \left(\left| \alpha \sum_{i=1}^{N} \left| \left[\mathbf{h}^{SR} \right]_i \right| \left| \left[\mathbf{h}^{RD} \right]_i \right| \right|^2 \right). \tag{5.28}$$

Let $\nu_i = \left| \left[\mathbf{h}^{SR} \right]_i \right| \left| \left[\mathbf{h}^{RD} \right]_i \right| \; \forall i \in \{1, \cdots, N\}$. Since received power cannot be greater than the transmit power, we have,

$$\frac{\alpha^2}{\sigma^2} \left(\sum_{i=1}^{N} \nu_i \right)^2 \leq 1 \tag{5.29}$$

Upper bound on the maximum number of IRS elements can be found from $\left(N \nu_{max} \right)^2 \leq \frac{\sigma^2}{\alpha^2}$ and received SNR over the reflection path with the largest gain has to be greater than 1(i.e $\gamma_s \nu_{max}^2 \geq 1$). On combining both we get $N^2 \leq \gamma_s \frac{\sigma^2}{\alpha^2}$. Thus, the maximum number of reflector elements is given by $N_{max} \leq \min\{\frac{1}{\nu_{max}} \sqrt{\frac{\sigma^2}{\alpha^2}}, \sqrt{\gamma_s \frac{\sigma^2}{\alpha^2}}\}$. In the absence of phase errors and when the SD link is in a permanent outage, we now solve the equation 5.6 using OP approximated from (5.7), where (5.8) and (5.9) can be evaluated using the following equations:

$$\mathbb{E}[\gamma_{IRS}^{npdl}] = \gamma_s \left[N \alpha^2 d_{sr}^{-\beta} d_{rd}^{-\beta} + \alpha^2 \frac{\pi^2 N(N-1)}{16} d_{sr}^{-\beta} d_{rd}^{-\beta} \right]. \tag{5.30}$$

$$\mathbb{E}[(\gamma_{IRS}^{npdl})^2] = \frac{N\alpha^4\gamma_s^2}{d_{sr}^{2\beta}d_{rd}^{2\beta}}\left[1 + 3N + \frac{3\pi^2(N-1)(2N-1)}{16} + \frac{(N-1)(N-2)(N-3)\pi^4}{256}\right]. \tag{5.31}$$

CHAPTER 6

SIMULATION RESULTS

In this section, we present the observations of simulation experiments to verify the results presented in Section 5.1. The simulation settings used in this paper are similar to [21] (shown in Fig 6.1). However, the focus in [21] was the ergodic capacity and hence they do not derive the CDF of γ_{IRS}. Here, for scenarios $\mathcal{S}_1$ and $\mathcal{S}_2$, the nodes **S** and **D** are located at the points $(0, 0)$ and $(90, 0)$ respectively and the **IRS** is located at the point (d, h). Throughout the simulations, we have taken amplitude coefficient α to be 1 (similar to [21]), b is chosen as 5, and γ_s to be 73 dB, unless mentioned otherwise. We consider three scenarios here, in the first scenario ($\mathcal{S}_1$), d_{sr} $\left(\sqrt{d^2 + h^2}\right)$ and d_{rd} $\left(\sqrt{(90 - d)^2 + h^2}\right)$ are chosen to be 95 metres and 10 metres, respectively. In the second scenario ($\mathcal{S}_2$), h is chosen to be 10 metres whereas d is varied across simulations. In the third scenario,($\mathcal{S}_3$), d_{sd}, d_{sr} and d_{rd} are chosen to be 200 metres, 250 metres and 100 metres, respectively. In the subsequent subsections, we compare the performance of the different approximations proposed for the cases with and without SD link.

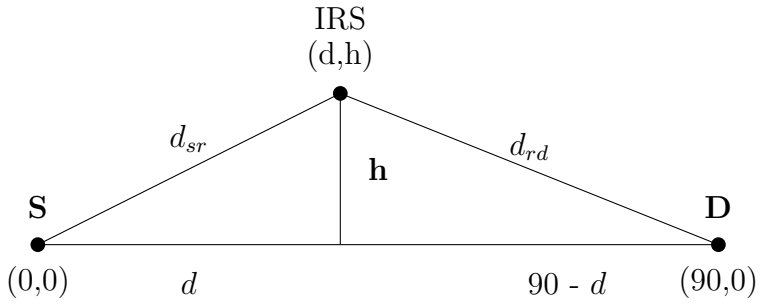

Figure 6.1: Simulation set up

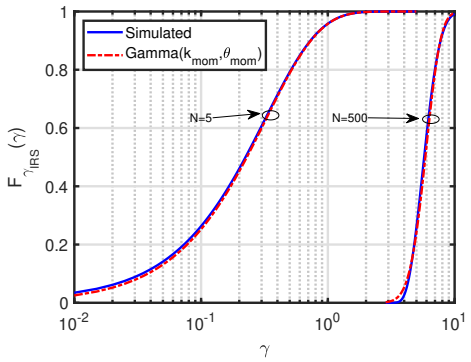

Figure 6.2: Comparison of the simulated CDF of γ_{IRS} with the CDF in (3.3) for $\mathcal{S}_1$.

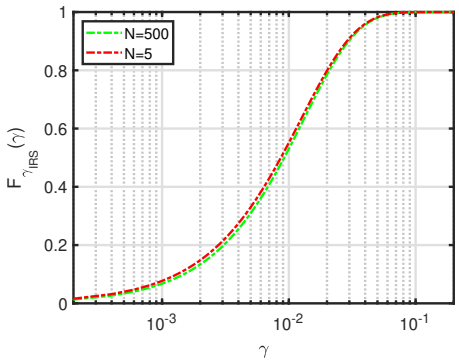

Figure 6.3: Comparison of the theoretical CDF of γ_{IRS} for $\mathcal{S}_3$.

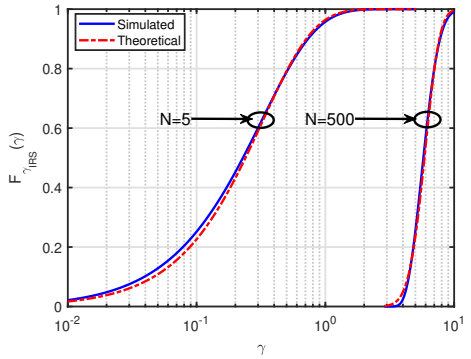

Figure 6.4: Comparison of the simulated CDF of γ_{IRS} with the CDF in (3.13) for $\mathcal{S}_1$.

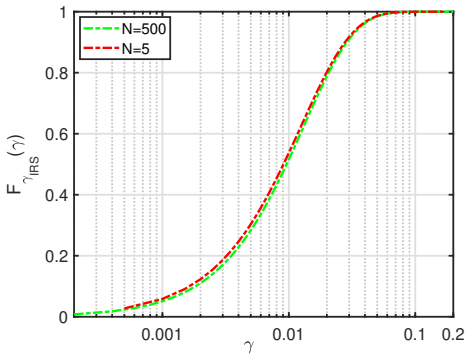

Figure 6.5: Comparison of the theoretical CDF of γ_{IRS} for $\mathcal{S}_3$.

$N = 5$	Method / Threshold	-10 dB	-5 dB	-2 dB	0 dB	2 dB	5 dB
	Simulated	0.2516	0.6206	0.8611	0.9575	0.9936	1.0000
	Gamma(k_{mom}, θ_{mom})	0.2525	0.6196	0.8608	0.9577	0.9937	1.0000
	Gamma(k_{kl}, θ_{kl})	0.2263	0.6115	0.8674	0.9639	0.9956	1.0000
$N = 50$	Method/Threshold	-10 dB	-5 dB	-2 dB	0 dB	2 dB	5 dB
	Simulated	0.0492	0.3599	0.6935	0.8813	0.9757	0.9997
	Gamma(k_{mom}, θ_{mom})	0.0717	0.3551	0.6856	0.8800	0.9769	0.9998
	Gamma(k_{kl}, θ_{kl})	0.0609	0.3413	0.6855	0.8858	0.9802	0.9998
$N = 500$	Method / Threshold	6 dB	7 dB	8 dB	9 dB	10 dB	11 dB
	Simulated	0.0226	0.2581	0.6523	0.9157	0.9916	0.9997
	Gamma(k_{mom}, θ_{mom})	0.0515	0.2452	0.6270	0.9221	0.9954	1.0000
	Gamma(k_{kl}, θ_{kl})	0.0507	0.2441	0.6273	0.9229	0.9956	1.0000

Table 6.1: Comparison of OP with SD link for $\mathcal{S}_1$ with varying N

6.0.1 Results with SD link

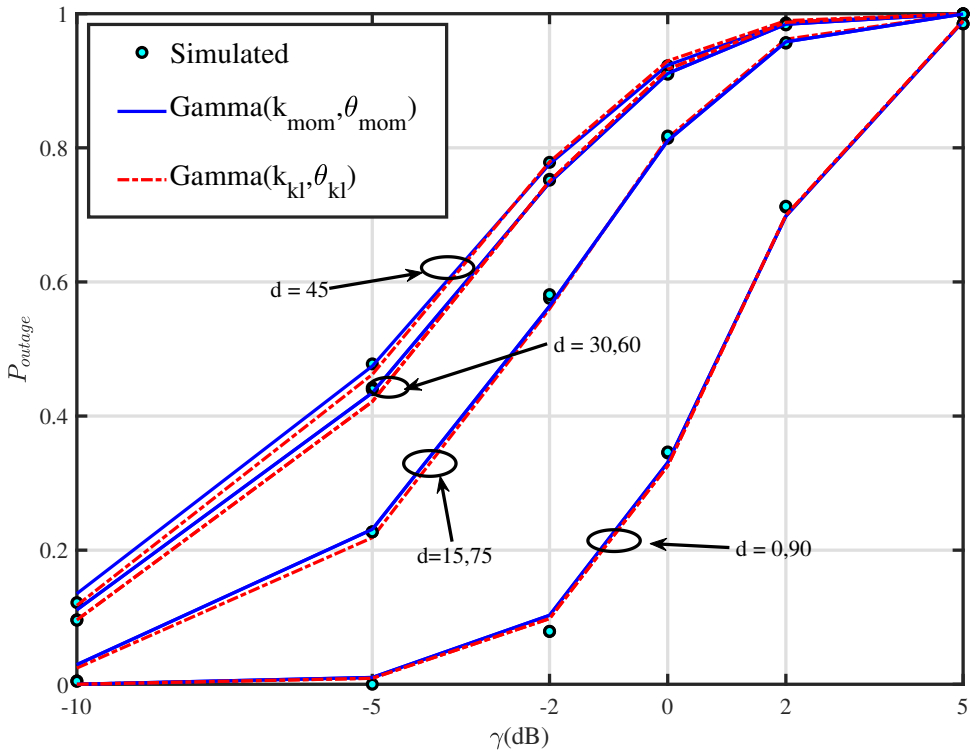

Figure 6.6: Impact of d on the OP with SD link for $\mathcal{S}_2$, $N = 150$

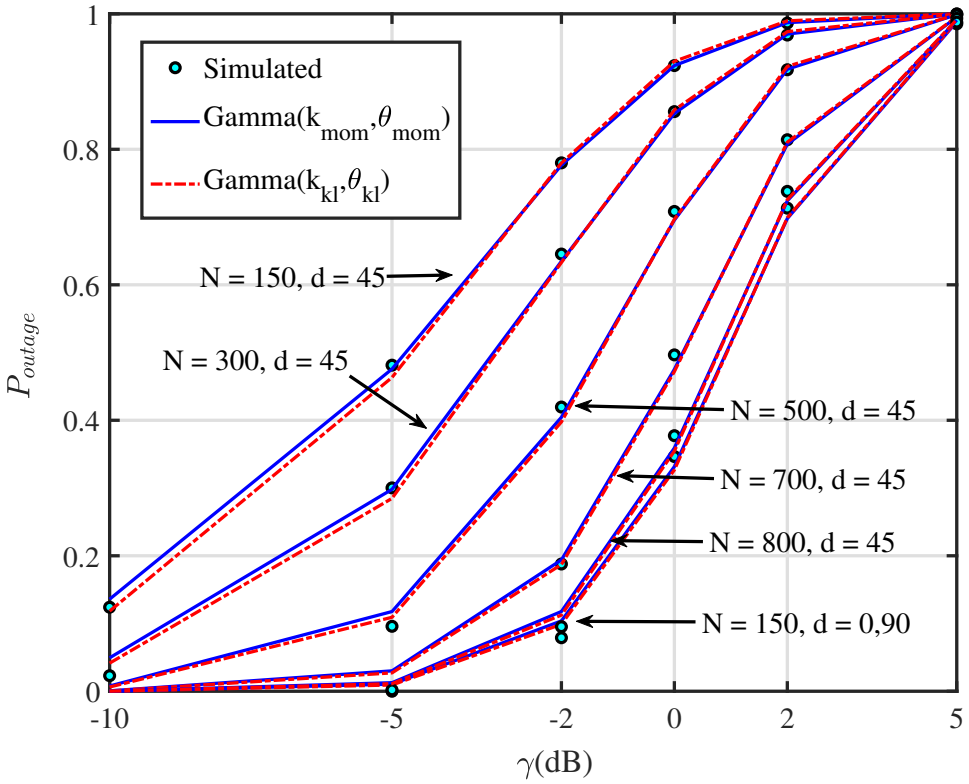

Figure 6.7: Impact of N on the OP with SD link for $\mathcal{S}_2$

In this sub-section, we examine the closeness between the simulated values of OP and the approximations proposed in Section 3.1.2, and 3.1.3. Here, figures 6.2 and 6.4 compares the CDF for N = 5 and N = 500 when the rest of the parameters are chosen according to S_1. One can note that the simulated and the approximate curves are matching perfectly for all values of γ. Next, in figures 6.3 and 6.5 we compare the CDF when the parameters are chosen according to S_2. In this case, the CDF curves for the case of N = 5 and N = 500 are very close, and for clarity we have included only the approximated curves in figures 6.3 and 6.5. Table 6.1 compares the OP obtained using (3.3), and (3.13) with the simulated values of OP for various values of N. Table 6.1 corroborates the fact that an increase in N improves the performance of an IRS system. One can also observe that the OP evaluated using all the three approximations are close to the simulated values. Table 6.2 demonstrates the effect of the number of quantization bits b on the OP. Here, one can observe that with a small number of bits itself one can achieve the performance of $b = \infty$ (*i.e.* the no phase error scenario). Furthermore, the

$N = 100$	Method / Threshold	-10 dB	-5 dB	-2 dB	0 dB	2 dB	5 dB
$b = 1$	Simulated	0.0166	0.2771	0.6240	0.8434	0.9648	0.9995
	Gamma(k_{mom}, θ_{mom})	0.0428	0.2772	0.6129	0.8398	0.9663	0.9997
	Gamma(k_{kl}, θ_{kl})	0.0358	0.2640	0.6103	0.8447	0.9700	0.9998
$b = 2$	Simulated	0	0.1390	0.4768	0.7493	0.9331	0.9987
	Gamma(k_{mom}, θ_{mom})	0.0132	0.1539	0.4619	0.7399	0.9345	0.9991
	Gamma(k_{kl}, θ_{kl})	0.0107	0.1438	0.4558	0.7422	0.9386	0.9993
$b = 10$	Simulated	0	0.0969	0.4183	0.7070	0.9164	0.9982
	Gamma(k_{mom}, θ_{mom})	0.0079	0.1180	0.4037	0.6936	0.9169	0.9987
	Gamma(k_{kl}, θ_{kl})	0.0064	0.1095	0.3967	0.6947	0.9211	0.9990
$b = \infty$	Simulated	0	0.0966	0.4178	0.7059	0.9160	0.9982
	Gamma(k_{mom}, θ_{mom})	0.0079	0.1180	0.4037	0.6936	0.9169	0.9987
	Gamma(k_{kl}, θ_{kl})	0.0064	0.1095	0.3967	0.6947	0.9211	0.9990

Table 6.2: Comparison of OP with SD link for $\mathcal{S}_1$ with varying b

improvement in performance with increasing b is not very large for $b > 2$. From Fig, 6.8 we can observe that the performance of an IRS system with 4 bits to represent the phase is very close to the performance of an IRS system with no phase error and N = 150. Hence for a practical system with large N, one will not need a very large number of bits to represent the phase. Depending upon the quality of service requirements, the system designer can choose the minimum value of b necessary to achieve the desired performance. Next, Fig. 6.6 demonstrates the impact of the position of the **IRS** with respect to the positions of **S** and **D**. Here one can observe the symmetry of the OP values for different IRS locations about the midpoint of the nodes **S** and **D**. We can also observe that farther the IRS from either of the nodes **S**/**D**, larger is the OP. Fig. 6.7 demonstrates the number of IRS elements required to match the performance of a system with $N = 150$ and $d = 0/90$ when the IRS is located at $d = 45$. From Fig. 6.7 it is clear that additional 650 reflector elements are needed when the **IRS** is placed mid-way between the nodes **S** and **D**, compared to a system with an IRS located above either of the nodes **S** or **D**. The authors of [16, 24, 30] also consider the presence of SD link in their analysis but do not take into account the phase error due to b bit phase representation.

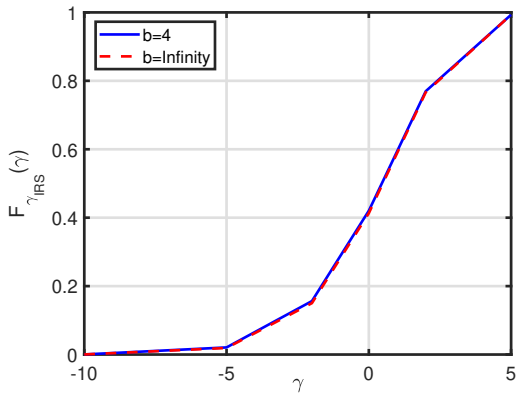

Figure 6.8: Impact of b on the OP for $N = 150$

6.0.2 Results without SD link

In this sub-section, we study the performance of an IRS-assisted system without an SD link. Table 6.3 demonstrates the variation in the OP for different values of b. Note that for the particular simulation setting considered we need 56 extra elements to achieve the performance comparable to a system without phase error when only one bit is used to represent the phase. Hence, one can either increase the number of elements or increase b to achieve better performance. Similarly, Fig. 6.9 elucidates the variation in the OP with respect to d. Here also we can observe that the farther the IRS from either of the nodes $\mathbf{S}/\mathbf{D}$, the larger is the OP. Furthermore, when the IRS was shifted by 8 meters *i.e.*, from $d = 15$ to $d = 23$, three extra bits were required to get similar performance in terms of OP.

Note that the authors of [22, 23, 29] also considers scenarios without SD link. In this context, we would like to point out that the work in [22] which approximates the square root of SNR as a Gamma RV gives OP expressions which are as tight as ours, however, extending their result to scenarios with SD link is not trivial. We had recovered the expressions given by [23] as special cases (presented in corollaries 1.2 and 1.3).

$N,\ b$	Method/ Threshold	-10 dB	-9 dB	-8 dB	-7 dB	-6 dB
$N = 156,\ b = 1$	Simulated	0.0067	0.1367	0.6287	0.9652	0.9995
	Gamma(k_{mom}, θ_{mom})	0.0084	0.1390	0.6257	0.9670	0.9998
	Gamma(k_{kl}, θ_{kl})	**0.0083**	**0.1384**	**0.6259**	**0.9673**	0.9998
$N = 100,\ b = 5$	Simulated	0.0064	0.1370	0.6370	0.9679	0.9997
	Gamma(k_{mom}, θ_{mom})	0.0080	0.1386	0.6321	**0.9697**	0.9998
	Gamma(k_{kl}, θ_{kl})	**0.0079**	**0.1380**	**0.6323**	0.9699	0.9998
$N = 100,\ b = \infty$	Simulated	0.0061	0.1326	0.6295	0.9663	0.9997
	Gamma(k_{mom}, θ_{mom})	0.0076	0.1344	0.6245	**0.9682**	0.9998
	Gamma(k_{kl}, θ_{kl})	**0.0047**	**0.1235**	**0.6332**	0.9711	0.9998

Table 6.3: Comparison of OP without SD link for $\mathcal{S}_1$ with varying b

N	d	b	Method/ Threshold	-10 dB	-5 dB	-2 dB	0 dB	2 dB	5 dB
5	0	1	Simulated	0.2600	0.6278	0.8651	0.9592	0.9940	1
			Gamma Approx.	0.2599	0.6284	0.8652	0.9592	0.9939	1
5	0	5	Simulated	0.2491	0.6186	0.8599	0.9571	0.9935	1
			Gamma Approx.	0.2487	0.6179	0.8597	0.9571	0.9935	1
5	45	1	Simulated	0.2768	0.6441	0.8730	0.9620	0.9945	1
			Gamma Approx.	0.2765	0.6432	0.8728	0.9621	0.9944	1
5	45	5	Simulated	0.2749	0.6412	0.8715	0.9619	0.9946	1
			Gamma Approx.	0.2744	0.6414	0.8718	0.9617	0.9944	1
150	0	1	Simulated	0	0.0759	0.3849	0.6812	0.9055	0.9978
			Gamma Approx.	0	0.0758	0.3849	0.6806	0.9055	0.9978
150	0	5	Simulated	0	2×10^{-5}	0.0790	0.3470	0.7137	0.9851
			Gamma Approx.	0	0	0.0791	0.3465	0.7130	0.9852
150	45	1	Simulated	0.1749	0.5431	0.8186	0.9407	0.9901	0.9999
			Gamma Approx.	0.1751	0.5431	0.8182	0.9403	0.9901	0.9999
150	45	5	Simulated	0.1232	0.4798	0.7795	0.9236	0.9864	0.9999
			Gamma Approx.	0.1232	0.4800	0.7793	0.9232	0.9863	0.9999

Table 6.4: OP with SD link for $\mathcal{S}_2$

N	d	b	Method/ Threshold	-45 dB	-40 dB	-35 dB	-30 dB	-25 dB	-20 dB
5	0	1	Simulated	0.0212	0.1809	0.6594	0.9779	0.9999	1
			Gamma Approx	0.0533	0.2183	0.641	0.9793	1	1
5	0	5	Simulated	0.0013	0.0364	0.3504	0.9041	0.9996	1
			Gamma Approx	0.0086	0.0652	0.3573	0.8968	0.9999	1
5	45	1	Simulated	0.9741	0.9999	1	1	1	1
			Gamma Approx	0.9753	1	1	1	1	1
5	45	5	Simulated	0.8916	0.9995	1	1	1	1
			Gamma Approx	0.8834	0.9999	1	1	1	1
N	d	b	Method/ Threshold	-10 dB	-9 dB	-8 dB	-7 dB	-6 dB	-5 dB
150	0	1	Simulated	0.0010	0.0405	0.3554	0.8545	0.9945	1
			Gamma Approx	0.0016	0.0439	0.3522	0.8539	0.9954	1
150	0	5	Simulated	0	0	0	0	0.0001	0.0247
			Gamma Approx	0	0	0	0	0.0002	0.0270
150	45	1	Simulated	1	1	1	1	1	1
			Gamma Approx	1	1	1	1	1	1
150	45	5	Simulated	1	1	1	1	1	1
			Gamma Approx	1	1	1	1	1	1

Table 6.5: OP without SD link for $\mathcal{S}_2$

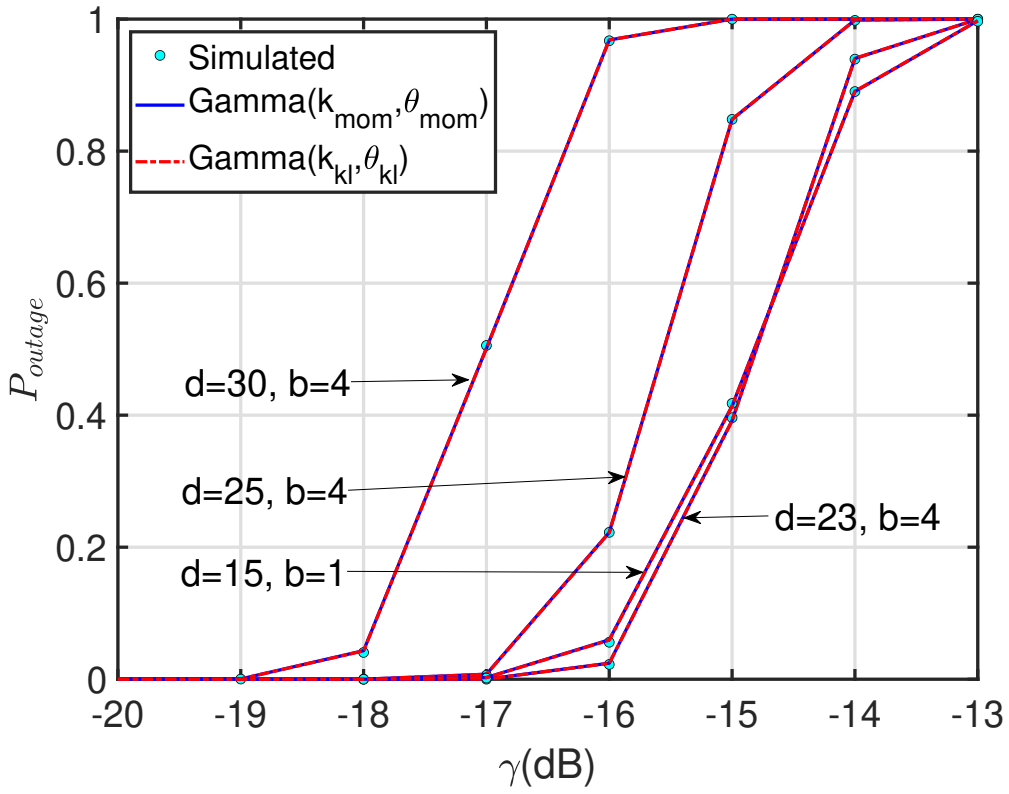

Figure 6.9: Impact of d on the OP without SD link for $\mathcal{S}_2$, $N = 150$.

Parameter	Impact of N	Impact of b	Impact of d
N is small	NA	less	less
N is large	NA	more	more
b is small	less	NA	less
b is large	more	NA	more
d close to **S**/**D**	more	more	NA
d away from **S**/**D**	less	less	NA

Table 6.6: Summary of impact of N, b and d on OP of

6.0.3 Key Inferences

In this sub-section, we discuss the key inferences drawn from the results presented in Section 6.0.1 and 6.0.2. Table 6.4 and 6.5 compares the values of OP for different values of N, d, and b for the scenarios with and without SD link, respectively. We have only included only the moment matching results for the Tables 6.4 and 6.5. From Table 6.4 we can observe that the reduction in OP as b increases from 1 to 5 is larger at $N = 150$ than at $N = 5$. Similar observations can also be made for the cases without SD link from Table 6.5. Thus, we conclude that an IRS with a small number of reflector elements is less sensitive to the number of bits used for representing the phase. Similarly, the values of OP in Tables 6.4 and 6.5 show that the impact of d on the OP is also larger for large values of N. Here, we can also observe that the impact of b and N on the OP increases as the IRS moves closer to either of the nodes S or D. Furthermore, we can observe from Tables 6.4 and 6.5 that the impact of phase errors is larger in the system without an SD link. We have summarised the above observations in Table 6.6.

CHAPTER 7

CONCLUSION AND FUTURE SCOPE

7.1 Conclusion

This paper studied the OP of an IRS-assisted communication system in the presence of phase errors due to quantization. We proposed two different approximations using 1) moment matching and, 2) KL divergence minimization. Our simulation results showed that the derived expressions are tight and can be reliably used for further analysis. The moment matching and KL divergence minimization results in simple closed-form expressions for the OP. Furthermore, the proposed approximations are highly useful in evaluating the effects of various system parameters on the OP. We have derived bounds to OP using Cauchy-Schwartz inequality and Upper bound to Bessel function of second kind. We also study the how large an IRS in order to provide reliable communication in the presence of phase error due to quantization at the IRS. We derived the no of reflector elements needed so that Outage Probability (OP) lie within an threshold and also optimized the Outage probability for an IRS given an upper bound on the IRS elements. In this work, we also studied the impact of the parameters like the number of bits available for quantization, the position of IRS w.r.t. source and destination and, the number of elements present at IRS.

7.2 Future scope

Since we have provided a tight approximation to the CDF, we believe that this can be used to study all other performance metrics which are functions of the CDF of SNR. It would be interesting future work to study a more general scenario where the source and/or thedestination is equipped with multiple antennas.

APPENDIX A

APPENDICES

A.1 Proof for lemma 1

Using (2.4) and (3.1), the OP for threshold γ can be evaluated as

$$P_{outage} = \mathbb{P}\left(\gamma_s|(|h^{SD}| + \alpha\sum_{i=1}^{N}|[\mathbf{h}^{SR}]_i||[\mathbf{h}^{RD}]_i|e^{j\Phi_i})|^2 \leq \gamma\right). \tag{A.1}$$

Let $|h^{SD}|, |[\mathbf{h}^{SR}]_i|$ and $|[\mathbf{h}^{RD}]_i|$ be denoted by $g_{SD}, [\mathbf{g}_{SR}]_i$ and $[\mathbf{g}_{RD}]_i$ respectively. After some algebraic manipulations, we can re-write (A.1) as

$$\begin{aligned} P_{outage} &= \mathbb{P}\left(\gamma_s\left(g_{SD} + \alpha\sum_{i=1}^{N}[\mathbf{g}_{SR}]_i[\mathbf{g}_{RD}]_i\cos(\Phi_i)\right)^2 + \gamma_s\left(\alpha\sum_{i=1}^{N}[\mathbf{g}_{SR}]_i[\mathbf{g}_{RD}]_i\sin(\Phi_i)\right)^2 \leq \gamma\right) \\ &= \mathbb{P}\left(\left(\sqrt{\gamma_s}g_{SD} + \mathbf{C}^T\mathbf{X}\right)^2 + \left(\mathbf{S}^T\mathbf{X}\right)^2 \leq \gamma\right) \end{aligned} \tag{A.2}$$

where $\mathbf{X} = \left[\sqrt{\gamma_s}[\mathbf{g}_{SR}]_1[\mathbf{g}_{RD}]_1 \ldots \sqrt{\gamma_s}[\mathbf{g}_{SR}]_N[\mathbf{g}_{RD}]_N\right]$, $\mathbf{C} = [\alpha\cos(\Phi_1), \ldots, \alpha\cos(\Phi_N)]^T$ and $\mathbf{S} = [\alpha\sin(\Phi_1)\ldots\alpha\sin(\Phi_N)]^T$. Now, the RV of interest is $Y = \left(\sqrt{\gamma_s}g_{SD} + \mathbf{C}^T\mathbf{X}\right)^2 + \left(\mathbf{S}^T\mathbf{X}\right)^2$. Note that Y is the sum of the square of two RVs, one of which is again a sum of N random variables ($\mathbf{S}^T\mathbf{X}$, where each X_i is a double Rayleigh RV and Φ_i is a uniformly distributed RV over the interval $[-2^{-b}\pi, 2^{-b}\pi]$). To the best of our knowledge, characterising the p.d.f. of this sum is not straight forward and is not available in the open literature. Similarly, characterising the distribution of the other term *i.e.*$\sqrt{\gamma_s}g_{SD} + \mathbf{C}^T\mathbf{X}$ is also difficult. To proceed further, we first derive the conditional CDF of γ_{IRS} for a particular value of $\mathbf{\Phi} = \boldsymbol{\phi}$ and $\mathbf{X} = \mathbf{x}$ and is given below:

$$\begin{aligned} P_{outage}|\left(\mathbf{\Phi} = \boldsymbol{\phi}, \mathbf{X} = \mathbf{x}\right) &= \mathbb{P}\left(\sqrt{\gamma_s}g_{SD} \leq \sqrt{\gamma - \left(\mathbf{s}^T\mathbf{x}\right)^2} - \mathbf{c}^T\mathbf{x}\right) \\ &= \left(1 - e^{\frac{-\left(\sqrt{\gamma-\left(\mathbf{s}^T\mathbf{x}\right)^2}-\mathbf{c}^T\mathbf{x}\right)^2 d_{sd}^{\beta}}{\gamma_s}}\right) \mathrm{U}\left(\sqrt{\gamma - \left(\mathbf{s}^T\mathbf{x}\right)^2} - \mathbf{c}^T\mathbf{x}\right) \end{aligned} \tag{A.3}$$

Now to evaluate the CDF of γ_{IRS}, we just need to evaluate the expectation of the R.H.S. of (A.3) with respect to the RVs $\mathbf{\Phi} = [\Phi_1, \ldots, \Phi_N]^T$ and $\mathbf{X} = [X_1, \ldots, X_N]^T$, both of which are multivariate vectors with i.i.d. entries. Their p.d.f.'s are as follows:

$$f_{X_i}(x_i) = \begin{cases} \frac{4d_{sr}^{\beta} d_{rd}^{\beta}}{\gamma_s} x_i \mathrm{K}_0 \left[\frac{2x_i}{\sqrt{\gamma_s} d_{sr}^{-\beta/2} d_{rd}^{-\beta/2}} \right] & \forall x_i \geq 0 \\ 0 & \text{else} \end{cases} \quad \text{and} \quad f_{\Phi_i}(\phi_i) = \begin{cases} \frac{2^b}{2\pi} & \frac{-\pi}{2^b} \leq \phi_i \leq \frac{\pi}{2^b} \\ 0 & \text{else.} \end{cases} \tag{A.4}$$

Thus, the CDF of γ_{IRS} is given by

$$P_{outage} = \int \cdots \int \left(1 - e^{\frac{-\left(\sqrt{\gamma - (\mathbf{s}^T\mathbf{x})^2} - \mathbf{c}^T\mathbf{x}\right)^2 d_{sd}^{\beta}}{\gamma_s}} \right) \mathrm{U}\left(\sqrt{\gamma - (\mathbf{s}^T\mathbf{x})^2} - \mathbf{c}^T\mathbf{x}\right) \prod_{i=1}^{N} f_{X_i}(x_i) f_{\Phi_i}(\phi_i) \, dx_1 d\phi_1 \ldots dx_N d\phi_N \tag{A.5}$$

The result in (3.2) follows by substituting the p.d.f. expressions from (A.4) in (A.5), and this completes the proof.

A.2 proof for Theorem 1

Here we derive the first and second moments of the RV γ_{IRS} given in (2.4). Let,

$$K := ||h^{SD}| + \alpha \sum_{i=1}^{N} |[\mathbf{h}^{SR}]_i||[\mathbf{h}^{RD}]_i| e^{j\Phi_i}|^2. \tag{A.6}$$

Now, the moments that we need to evaluate can be expressed as:

$$\mathbb{E}\left[\gamma_{IRS}\right] = \gamma_s \mathbb{E}\left[K\right], \tag{A.7}$$

$$\mathbb{E}\left[\gamma_{IRS}^2\right] = \gamma_s^2 \mathbb{E}\left[K^2\right]. \tag{A.8}$$

Note that K can be expanded as follows:

$$K = \underbrace{|h^{SD}|^2 + \alpha^2 \sum_{i=1}^{N} |[\mathbf{h}^{SR}]_i|^2 |\mathbf{h}^{RD}]_i|^2}_{A} + \underbrace{2\alpha |h^{SD}| \sum_{i=1}^{N} |[\mathbf{h}^{SR}]_i| |[\mathbf{h}^{RD}]_i| \cos(\Phi_i)}_{B} + \underbrace{2\alpha^2 \sum_{i=1}^{N-1} \sum_{k=i+1}^{N} |[\mathbf{h}^{SR}]_i| |[\mathbf{h}^{RD}]_i| |[\mathbf{h}^{SR}]_k| |[\mathbf{h}^{RD}]_k| \cos(\Phi_i - \Phi_k)}_{C} . \tag{A.9}$$

Hence the first and second moment of $K = A + B + C$ can be evaluated as follows:

$$\mathbb{E}[K] = \mathbb{E}[A] + \mathbb{E}[B] + \mathbb{E}[C] . \tag{A.10}$$

$$\mathbb{E}\left[K^2\right] = \mathbb{E}\left[A^2\right] + \mathbb{E}\left[B^2\right] + \mathbb{E}\left[C^2\right] + 2\mathbb{E}[AB] + 2\mathbb{E}[BC] + 2\mathbb{E}[AC] . \tag{A.11}$$

Next, in order to find the above moments, we plug in A, B, C and derive individual expectations assuming $s := \frac{\sin\left(\frac{\pi}{2^b}\right)}{\frac{\pi}{2^b}}$, $p := \frac{\sin\left(2\frac{\pi}{2^b}\right)}{2\frac{\pi}{2^b}}$. Let us find the first moments of RV A, B and C,

$$\mathbb{E}[A] = \mathbb{E}\left[|h^{SD}|^2 + \alpha^2 \sum_{i=1}^{N} |[\mathbf{h}^{SR}]_i|^2 |[\mathbf{h}^{RD}]_i|^2\right] = d_{sd}^{-\beta} + N\alpha^2 d_{sr}^{-\beta} d_{rd}^{-\beta}, \tag{A.12}$$

where $\mathbb{E}\left[|h^{ab}|^2\right] = d_{ab}^{-\beta}$, $a, b \in \{\mathbf{S}, \mathbf{R}, \mathbf{D}\}$.

$$\mathbb{E}[B] = \mathbb{E}\left[2\alpha |h^{SD}| \sum_{i=1}^{N} |[\mathbf{h}^{SR}]_i| |[\mathbf{h}^{RD}]_i| \cos(\Phi_i)\right] = \frac{N\alpha\pi^{\frac{3}{2}}}{4} d_{sr}^{\frac{-\beta}{2}} d_{rd}^{\frac{-\beta}{2}} d_{sd}^{\frac{-\beta}{2}} s, \tag{A.13}$$

where $\mathbb{E}[\cos(\Phi_i)] = \frac{\sin\left(\frac{\pi}{2^b}\right)}{\frac{\pi}{2^b}} = s$, $\mathbb{E}\left[|h^{ab}|\right] = \frac{\sqrt{\pi}}{2} d_{ab}^{-\beta/2}$, $a, b \in \{\mathbf{S}, \mathbf{R}, \mathbf{D}\}$.

$$\begin{aligned} \mathbb{E}[C] &= \mathbb{E}\left[2\alpha^2 \sum_{i=1}^{N-1} \sum_{k=i+1}^{N} |[\mathbf{h}^{SR}]_i| |[\mathbf{h}^{RD}]_i| |[\mathbf{h}^{SR}]_k| |[\mathbf{h}^{RD}]_k| \cos(\Phi_i - \Phi_k)\right] \\ &= \frac{\pi^2 \alpha^2}{8} d_{sr}^{-\beta} d_{rd}^{-\beta} \frac{N(N-1)}{2} s^2, \end{aligned} \tag{A.14}$$

where $\mathbb{E}\left[\cos\left(\Phi_i - \Phi_k\right)\right] = \left(\frac{\sin\left(\frac{\pi}{2^b}\right)}{\frac{\pi}{2^b}}\right)^2 = s^2$. Similarly, the second moments of the RV A, B, C are derived as follows,

$$\begin{aligned}\mathbb{E}\left[A^2\right] &= \mathbb{E}\left[\left(|h^{SD}|^2 + \alpha^2 \sum_{i=1}^{N} |[\mathbf{h}^{SR}]_i|^2 |[\mathbf{h}^{RD}]_i|^2\right)^2\right] \\ &= 2d_{sd}^{-2\beta} + 2\alpha^2 N d_{sd}^{-\beta} d_{sr}^{-\beta} d_{rd}^{-\beta} + \alpha^4 \left(3N + N^2\right) d_{sr}^{-2\beta} d_{rd}^{-2\beta},\end{aligned} \tag{A.15}$$

where $\mathbb{E}\left[|h^{ab}|^4\right] = 2d_{ab}^{-2\beta}$, $a, b \in \{\mathbf{S}, \mathbf{R}, \mathbf{D}\}$.

$$\begin{aligned}\mathbb{E}[B^2] =& \mathbb{E}\left[\left(2\alpha |h^{SD}| \sum_{i=1}^{N} |[\mathbf{h}^{SR}]_i| |[\mathbf{h}^{RD}]_i| \cos(\Phi_i)\right)^2\right] \\ &= 4\alpha^2 \mathbb{E}[|h^{SD}|^2] \left[\sum_{i=1}^{N} \mathbb{E}\left[|[\mathbf{h}^{SR}]_i|^2\right] \mathbb{E}[|[\mathbf{h}^{RD}]_i|^2] \mathbb{E}[\cos^2(\Phi_i)]\right. \\ &\left. + 2 \sum_{i=1}^{N-1} \sum_{j=i+1}^{N} \mathbb{E}[|[\mathbf{h}^{SR}]_i|] \mathbb{E}[|[\mathbf{h}^{RD}]_i|] \mathbb{E}[|[\mathbf{h}^{SR}]_j|] \mathbb{E}[|[\mathbf{h}^{RD}]_i|] \mathbb{E}[\cos(\Phi_i)] \mathbb{E}[\cos(\Phi_j)]\right] \\ &= 4\alpha^2 d_{sr}^{-\beta} d_{rd}^{-\beta} d_{sd}^{-\beta} \left[N\left(\frac{1+p}{2}\right) + \frac{N\left(N-1\right) s^2 \pi^2}{16}\right],\end{aligned} \tag{A.16}$$

where $\mathbb{E}\left[\cos^2(\Phi_i)\right] = \left[\frac{1}{2} + \frac{2^b}{2\pi} \sin(\frac{\pi}{2^b}) \cos(\frac{\pi}{2^b})\right] = \frac{1+p}{2}$.

$$\begin{aligned}\mathbb{E}[C^2] =& \mathbb{E}\left[\left(2\alpha^2 \sum_{i=1}^{N-1} \sum_{k=i+1}^{N} |[\mathbf{h}^{SR}]_i| |[\mathbf{h}^{RD}]_i| |[\mathbf{h}^{SR}]_k| |[\mathbf{h}^{RD}]_k| \cos(\Phi_i - \Phi_k)\right)^2\right] \\ &= 4\alpha^4 \sum_{i=1}^{N-1} \sum_{k=i+1}^{N} \mathbb{E}^2\left[|[\mathbf{h}^{SR}]_i|^2\right] \mathbb{E}^2\left[|[\mathbf{h}^{RD}]_i|^2\right] \mathbb{E}\left[\cos^2(\Phi_i - \Phi_k))\right] \\ &+ 4\alpha^4 \sum_{j=1}^{N} \sum_{\substack{i=1 \\ i\neq j\neq k\neq l}}^{N-1} \sum_{k=i+1}^{N} \sum_{l=j+1}^{N} \left[\mathbb{E}^4\left[|[\mathbf{h}^{SR}]_i|\right] \mathbb{E}^4\left[|[\mathbf{h}^{RD}]_i|\right] \mathbb{E}^2\left[\cos\left(\Phi_i - \Phi_k\right)\right]\right. \\ &+ 4\alpha^4 \sum_{j=1}^{N} \sum_{\substack{i=1 \\ j=i\neq k\neq l}}^{N-1} \sum_{k=i+1}^{N} \sum_{l=j+1}^{N} \left[\mathbb{E}\left[|[\mathbf{h}^{SR}]_k|\right] \mathbb{E}\left[|[\mathbf{h}^{RD}]_k|\right] \mathbb{E}\left[|[\mathbf{h}^{SR}]_l|\right] \mathbb{E}\left[|[\mathbf{h}^{RD}]_l|\right]\right. \\ &\left.\left. \mathbb{E}\left[|[\mathbf{h}^{SR}]_i|^2\right] \mathbb{E}\left[|[\mathbf{h}^{RD}]_i|^2\right] \mathbb{E}\left[\cos(\Phi_i - \Phi_k) \cos(\Phi_i - \Phi_l)\right]\right],\end{aligned}$$

Using $\mathbb{E}\left[\cos^2(\Phi_i - \Phi_k)\right] = \frac{1}{2} + \frac{1}{2}\left(\frac{\sin\left(2\frac{\pi}{2^b}\right)}{2\frac{\pi}{2^b}}\right)^2 = \frac{1+p^2}{2}$ and $\mathbb{E}\left[\cos\left(\Phi_i - \Phi_k\right) \cos(\Phi_i - \Phi_l)\right] = \frac{1}{2}s^2 + \frac{1}{2}ps^2$, above equation can be written as

$$\mathbb{E}\left[C^2\right] = N(N-1)\alpha^4 d_{sr}^{-2\beta} d_{rd}^{-2\beta} \left[1 + p^2 + \frac{(N-2)(N-3)\pi^4 s^4}{256} + \frac{(N-2)\pi^2 s^2}{4}\left(\frac{1+p}{2}\right)\right]. \tag{A.17}$$

Next, we derive the expectation of RV's AB, BC and AC,

$$\mathbb{E}[AB] = \mathbb{E}\left[\left(|h^{SD}|^2 + \alpha^2 \sum_{i=1}^{N} |[\mathbf{h}^{SR}]_i|^2 |[\mathbf{h}^{RD}]_i|^2\right) \times \left(2\alpha |h^{SD}| \sum_{i=1}^{N} |[\mathbf{h}^{SR}]_i| |[\mathbf{h}^{RD}]_i| \cos(\Phi_i)\right)\right], \tag{A.18}$$

Since each of the link are independent, we now evaluate the expectation as,

$$\begin{aligned}\mathbb{E}\left[AB\right] =& 2\alpha \mathbb{E}\left[|h^{SD}|^3\right] \sum_{i=1}^{N} \mathbb{E}\left[|[\mathbf{h}^{SR}]_i|\right] \mathbb{E}\left[|[\mathbf{h}^{RD}]_i|\right] \mathbb{E}\left[\cos(\Phi_i)\right] \\ &+ 4\alpha^3 \mathbb{E}\left[|h^{SD}|\right] \sum_{j=1}^{N-1} \sum_{i=j+1}^{N} \mathbb{E}\left[|[\mathbf{h}^{SR}]_i|^2\right] \mathbb{E}\left[|[\mathbf{h}^{RD}]_i|^2\right] \mathbb{E}\left[|[\mathbf{h}^{SR}]_i|\right] \mathbb{E}\left[|[\mathbf{h}^{RD}]_i|\right] \mathbb{E}\left[\cos(\Phi_i)\right] \\ &+ 2\alpha^3 \mathbb{E}\left[|h^{SD}|\right] \sum_{i=1}^{N} \mathbb{E}\left[|[\mathbf{h}^{SR}]_i|^3\right] \mathbb{E}\left[|[\mathbf{h}^{RD}]_i|^3\right] \mathbb{E}\left[\cos(\Phi_i)\right]),\end{aligned} \tag{A.19}$$

Substituting the values of expectations where $\mathbb{E}[|h^{ab}|^3] = \frac{3}{4}\sqrt{\pi} d_{ab}^{-3\beta/2}$, $a, b \in \{\mathbf{S}, \mathbf{R}, \mathbf{D}\}$, we have

$$\mathbb{E}[AB] = \alpha \frac{3\pi^{\frac{3}{2}}}{8} d_{sd}^{-3\beta/2} d_{sr}^{-\beta/2} d_{rd}^{-\beta/2} (Ns) + \alpha^3 \frac{(4N+5)\,\pi^{\frac{3}{2}}}{16} d_{sd}^{-\beta/2} d_{sr}^{-3\beta/2} d_{rd}^{-3\beta/2} (Ns). \tag{A.20}$$

Next we consider the expectation of the term BC,

$$\begin{aligned}\mathbb{E}[BC] =& \mathbb{E}\left[2\alpha |h_{SD}| \sum_{i=1}^{N} |[\mathbf{h}_{SR}]_i| |[\mathbf{h}_{RD}]_i| \cos(\Phi_i) \times \right. \\ & \left. 2\alpha^2 \sum_{i=1}^{N-1} \sum_{k=i+1}^{N} |[\mathbf{h}_{SR}]_i| |[\mathbf{h}_{RD}]_i| |[\mathbf{h}_{SR}]_k| |[\mathbf{h}_{RD}]_k| (\cos(\Phi_i - \Phi_k))\right],\end{aligned} \tag{A.21}$$

As all the channel coefficients are assumed to be independent of each other, we can write the above equation as

$$\begin{aligned}\mathbb{E}[BC] =& 4\alpha^3 \frac{\sqrt{\pi}}{2} d_{sd}^{-\beta/2} (\frac{\sqrt{\pi}}{2} d_{sr}^{-\beta/2})^3 (\frac{\sqrt{\pi}}{2} d_{rd}^{-\beta/2})^3 \sum_{j=1}^{N} \sum_{\substack{i=1 \\ i\neq j\neq k}}^{N-1} \sum_{k=i+1}^{N} \mathbb{E}\left[\cos(\Phi_j)(\cos(\Phi_i)\cos(\Phi_k))\right] \\ &+ 4\alpha^3 \frac{\sqrt{\pi}}{2} d_{sd}^{-\beta/2} d_{sr}^{-\beta} d_{rd}^{-\beta} \frac{\sqrt{\pi}}{2} d_{sr}^{-\beta/2} \frac{\sqrt{\pi}}{2} d_{rd}^{-\beta/2} \sum_{i=1}^{N-1} \sum_{k=i+1}^{N} \mathbb{E}\left[\cos(\Phi_i)(\cos(\Phi_i)\cos(\Phi_k))\right] \\ &+ 4\alpha^3 \frac{\sqrt{\pi}}{2} d_{sd}^{-\beta/2} d_{sr}^{-\beta} d_{rd}^{-\beta} \frac{\sqrt{\pi}}{2} d_{sr}^{-\beta/2} \frac{\sqrt{\pi}}{2} d_{rd}^{-\beta/2} \sum_{i=1}^{N-1} \sum_{k=i+1}^{N} \mathbb{E}\left[\cos(\Phi_k)(\cos(\Phi_i)\cos(\Phi_k))\right],\end{aligned} \tag{A.22}$$

By substituting expressions for expectations we get,

$$\mathbb{E}[BC] = \frac{\alpha^3\pi^{7/2}d_{sd}^{-\frac{\beta}{2}}d_{sr}^{-3\frac{\beta}{2}}d_{rd}^{-3\frac{\beta}{2}}}{32}\frac{N(N-1)(N-2)}{2}s^3 + \frac{\alpha^3\pi^{3/2}N(N-1)}{2}d_{sd}^{-\frac{\beta}{2}}d_{sr}^{-3\frac{\beta}{2}}d_{rd}^{-3\frac{\beta}{2}}s\frac{(1+p)}{2}. \tag{A.23}$$

Finally, we evaluate the expectation of the last term AC,

$$\mathbb{E}[AC] = \mathbb{E}\left[\left(|h^{SD}|^2 + \alpha^2\sum_{i=1}^{N}|[\mathbf{h}^{SR}]_i|^2|[\mathbf{h}^{RD}]_i|^2\right)\times \left(2\alpha^2\sum_{i=1}^{N-1}\sum_{k=i+1}^{N}|[\mathbf{h}^{SR}]_i||[\mathbf{h}^{RD}]_i||[\mathbf{h}^{SR}]_k||[\mathbf{h}^{RD}]_k|\cos(\Phi_i-\Phi_k)\right)\right], \tag{A.24}$$

we can write the above equation as

$$\mathbb{E}[AC] = \mathbb{E}[|h^{SD}|^2]\mathbb{E}[C] \tag{A.25}$$

$$+2\alpha^4\sum_{i=1}^{N-1}\sum_{k=i+1}^{N}\mathbb{E}[|[\mathbf{h}^{SR}]_j|^3]\mathbb{E}[|[\mathbf{h}^{RD}]_j|^3]\mathbb{E}[|[\mathbf{h}^{SR}]_j|]\mathbb{E}[|[\mathbf{h}^{RD}]_j|]\mathbb{E}[\cos(\Phi_i-\Phi_k)]$$
$$+4\alpha^4\sum_{j=1}^{N}\sum_{\substack{i=1\\ i\neq j\neq k}}^{N-1}\sum_{k=i+1}^{N}\mathbb{E}[|[\mathbf{h}^{SR}]_j|^2]\mathbb{E}[|[\mathbf{h}^{RD}]_j|^2]\mathbb{E}[|[\mathbf{h}^{SR}]_j|]^2\mathbb{E}[|[\mathbf{h}^{RD}]_j|]^2\mathbb{E}[\cos(\Phi_i-\Phi_k)], \tag{A.26}$$

Substituting for the expectation, we get

$$\mathbb{E}[AC] = d_{sd}^{-\beta}\mathbb{E}[C] + \alpha^4\frac{(2N+5)\pi^2}{16}d_{sr}^{-2\beta}d_{sr}^{-2\beta}\frac{(N)(N-1)}{2}s^2. \tag{A.27}$$

Thus, the first and second moments are given by

$$\mathbb{E}[\gamma_{IRS}] = \gamma_s[N\alpha^2 d_{sr}^{-\beta}d_{rd}^{-\beta} + d_{sd}^{-\beta} + \alpha\frac{\pi^{\frac{3}{2}}}{4}d_{sr}^{\frac{-\beta}{2}}d_{rd}^{\frac{-\beta}{2}}d_{sd}^{\frac{-\beta}{2}}Ns + \alpha^2\frac{\pi^2}{8}d_{sr}^{-\beta}d_{rd}^{-\beta}\frac{N(N-1)}{2}s^2]. \tag{A.28}$$

$$\mathbb{E}\left[\gamma_{IRS}^2\right] = \gamma_s^2 \Bigg[2d_{sd}^{-2\beta} + \frac{3Ns\alpha\pi^{3/2}}{4} d_{sd}^{-3\beta/2} d_{sr}^{-\beta/2} d_{rd}^{-\beta/2} + N\alpha^2 d_{sr}^{-\beta} d_{rd}^{-\beta} d_{sd}^{-\beta} \left[\frac{3(N-1)\pi^2 s^2}{8} + 4 + 2p \right]$$
$$+ N\alpha^4 d_{sr}^{-2\beta} d_{rd}^{-2\beta} 2\left[N+1\right]$$
$$+ N\alpha^4 d_{sr}^{-2\beta} d_{rd}^{-2\beta} (N-1) \left[p^2 + \frac{(N-2)(N-3)\pi^4 s^4}{256} + \frac{\pi^2 s^2}{16} \left[2p(N-2) + 4N + 1\right] \right]$$
$$+ N\alpha^3 \pi^{3/2} d_{sd}^{-\beta/2} d_{sr}^{-3\beta/2} d_{rd}^{-3\beta/2} \left[(4N+5)\frac{s}{8} + \frac{(N-1)(N-2)\pi^2 s^3}{32} + (N-1)s\left(\frac{1}{2} + \frac{p}{2}\right) \right] \Bigg]. \tag{A.29}$$

where $s = \frac{\sin\left(\frac{\pi}{2^b}\right)}{\frac{\pi}{2^b}}, p = \frac{\sin\left(\frac{2\pi}{2^b}\right)}{\frac{2\pi}{2^b}}$ This completes the proof.

A.3 Proof for Theorem 2

Here, we proceed with steps similar to the KL divergence minimization used by the authors of [37]. Let $p(\gamma)$ and $q(\gamma)$ respectively represent the pdf of the SNR and the Gamma distribution that minimizes the KL divergence between $p(\gamma)$ and all the Gamma distributions i.e.,

$$q(\gamma) = \underset{q(\gamma)}{\operatorname{argmin}} \ \mathrm{KL}(p(\gamma) \| q(\gamma)) = \underset{q(\gamma)}{\operatorname{argmax}} \int p(\gamma)[\ln(q(\gamma)) - \ln(p(\gamma))] d\gamma,$$
$$= \underset{q(\gamma)}{\operatorname{argmax}} \int p(\gamma) \ln(q(\gamma)) d\gamma. \tag{A.30}$$

Here we have, $q(\gamma) = \frac{\theta_{kl}^{-k_{kl}}}{\Gamma[k_{kl}]} \gamma^{k_{kl}-1} \exp\left(\frac{-\gamma}{\theta_{kl}}\right)$, where k_{kl}, θ_{kl} are respectively the shape and scale parameter of the Gamma distribution. Thus,

$$q(\gamma) = \underset{q(\gamma)}{\operatorname{argmax}} \int p(\gamma) \left(-k_{kl} \log(\theta_{kl}) - \log(\Gamma[k_{kl}]) + (k_{kl}-1)\log(\gamma) - \frac{\gamma}{\theta_{kl}} \right) d\gamma \tag{A.31}$$

$$= \underset{q(\gamma)}{\operatorname{argmax}} - k_{kl} \log(\theta_{kl}) - \log(\Gamma[k_{kl}]) + (k_{kl}-1)\mathbb{E}[\log(\gamma)] - \frac{\mathbb{E}[\gamma]}{\theta_{kl}}. \tag{A.32}$$

Now, the parameters k_{kl} and θ_{kl} can be identified by differentiating (A.32) with respect to k_{kl} and θ_{kl} and then equating each of the expression to zero. Thus, we

have

$$\mathbb{E}[\log(\gamma_{IRS})] = \log(\theta_{kl}) + \psi(k_{kl}), \tag{A.33}$$

$$\mathbb{E}[\gamma_{IRS}] = k_{kl} \times \theta_{kl}. \tag{A.34}$$

One can observe that (A.33) and (A.34) are equivalent to matching the first moment of γ_{IRS} and the first moment of $\log(\gamma_{IRS})$ to the corresponding moments of a gamma RV. Thus, the probability of outage for a threshold γ is obtained by evaluating the CDF of the Gamma RV with parameters k_{kl} and θ_{kl} at γ. The corresponding expression is given in (3.13).

A.4 proof for Theorem 3

Here, we derive the first and second moments of the RV γ_{IRS} given in (2.4). Let,

$$K := ||h^{SD}| + \alpha \sum_{i=1}^{N} |[\mathbf{h}^{SR}]_i||[\mathbf{h}^{RD}]_i| e^{j\Phi_i}|^2. \tag{A.35}$$

Now, the moments that we need to evaluate can be expressed as $\mathbb{E}[\gamma_{IRS}] = \gamma_s \mathbb{E}[K]$, $\mathbb{E}[\gamma_{IRS}^2] = \gamma_s^2 \mathbb{E}[K^2]$. Note that K can be expanded as follows:

$$K = \underbrace{|h^{SD}|^2 + \alpha^2 \sum_{i=1}^{N} |[\mathbf{h}^{SR}]_i|^2 |[\mathbf{h}^{RD}]_i|^2}_{A} + \underbrace{2\alpha |h^{SD}| \sum_{i=1}^{N} |[\mathbf{h}^{SR}]_i||[\mathbf{h}^{RD}]_i| \cos(\Phi_i)}_{B} +$$
$$\underbrace{2\alpha^2 \sum_{i=1}^{N-1} \sum_{k=i+1}^{N} |[\mathbf{h}^{SR}]_i||[\mathbf{h}^{RD}]_i||[\mathbf{h}^{SR}]_k||[\mathbf{h}^{RD}]_k| \cos(\Phi_i - \Phi_k)}_{C}. \tag{A.36}$$

Hence, the first and second moment of K can be evaluated as $\mathbb{E}[K] = \mathbb{E}[A] + \mathbb{E}[B] + \mathbb{E}[C]$ and $\mathbb{E}[K^2] = \mathbb{E}[A^2] + \mathbb{E}[B^2] + \mathbb{E}[C^2] + 2\mathbb{E}[AB] + 2\mathbb{E}[BC] + 2\mathbb{E}[AC]$. Next, in order to find the above moments, we plug in A, B, C and derive individual expectations assuming $s := \frac{\sin\left(\frac{\pi}{2^b}\right)}{\frac{\pi}{2^b}}$, $p := \frac{\sin\left(2\frac{\pi}{2^b}\right)}{2\frac{\pi}{2^b}}$, $m_1^{ab} := \mathbb{E}\left[|h^{ab}|\right]$, $m_2^{ab} := \mathbb{E}\left[|h^{ab}|^2\right]$, $m_3^{ab} := \mathbb{E}\left[|h^{ab}|^3\right]$, $m_4^{ab} := \mathbb{E}\left[|h^{ab}|^4\right]$. Let us find the first moments of RV's A, B,

and C,

$$\mathbb{E}\left[A\right] = \mathbb{E}\left[|h^{SD}|^2 + \alpha^2 \sum_{i=1}^{N} |[\mathbf{h}^{SR}]_i|^2 |[\mathbf{h}^{RD}]_i|^2\right] = m_2^{sd} + N\alpha^2 m_2^{sr} m_2^{rd}, \tag{A.37}$$

where $\mathbb{E}\left[|h^{ab}|^2\right] = m_2^{ab}$, $a, b \in \{\mathbf{S}, \mathbf{R}, \mathbf{D}\}$.

$$\begin{aligned} \mathbb{E}\left[B\right] &= \mathbb{E}\left[2\alpha |h^{SD}| \sum_{i=1}^{N} |[\mathbf{h}^{SR}]_i| |[\mathbf{h}^{RD}]_i| \cos\left(\Phi_i\right)\right] \\ &= 2Ns\ \alpha m_1^{sd} m_1^{sr} m_1^{rd}, \end{aligned} \tag{A.38}$$

where $\mathbb{E}\left[\cos(\Phi_i)\right] = \frac{\sin\left(\frac{\pi}{2^b}\right)}{\frac{\pi}{2^b}} = s$, $\mathbb{E}\left[|h^{ab}|\right] = m_1^{ab}$, $a, b \in \{\mathbf{S}, \mathbf{R}, \mathbf{D}\}$.

$$\begin{aligned} \mathbb{E}[C] &= \mathbb{E}\left[2\alpha^2 \sum_{i=1}^{N-1} \sum_{k=i+1}^{N} |[\mathbf{h}^{SR}]_i| |[\mathbf{h}^{RD}]_i| |[\mathbf{h}^{SR}]_k| |[\mathbf{h}^{RD}]_k| \cos\left(\Phi_i - \Phi_k\right)\right] \\ &= 2\alpha^2 (m_1^{sr})^2 (m_1^{rd})^2 \frac{N(N-1)}{2} s^2, \end{aligned} \tag{A.39}$$

where $\mathbb{E}\left[\cos\left(\Phi_i - \Phi_k\right)\right] = \left(\frac{\sin\left(\frac{\pi}{2^b}\right)}{\frac{\pi}{2^b}}\right)^2 = s^2$. Similarly, the second moments of the RV A, B, and C are derived as follows,

$$\begin{aligned} \mathbb{E}\left[A^2\right] &= \mathbb{E}\left[\left(|h^{SD}|^2 + \alpha^2 \sum_{i=1}^{N} |[\mathbf{h}^{SR}]_i|^2 |[\mathbf{h}^{RD}]_i|^2\right)^2\right] \\ &= m_4^{sd} + 2\alpha^2 N m_2^{sr} m_2^{rd} m_2^{sd} + N\alpha^4 m_4^{sr} m_4^{rd} + 2\alpha^4 \frac{N(N-1)}{2} (m_2^{sr})^2 (m_2^{rd})^2, \end{aligned} \tag{A.40}$$

where $\mathbb{E}\left[|h^{ab}|^4\right] = m_4^{ab}$, $a, b \in \{\mathbf{S}, \mathbf{R}, \mathbf{D}\}$.

$$\begin{aligned} \mathbb{E}[B^2] =& \mathbb{E}\left[\left(2\alpha |h^{SD}| \sum_{i=1}^{N} |[\mathbf{h}^{SR}]_i| |[\mathbf{h}^{RD}]_i| \cos(\Phi_i)\right)^2\right] \\ &= 4\alpha^2 m_2^{sd} \left[N m_2^{sr} m_2^{rd} [\frac{1+p}{2}] + 2s^2 \frac{N(N-1)}{2} (m_2^{sr})^2 (m_2^{rd})^2\right], \end{aligned} \tag{A.41}$$

where $\mathbb{E}\left[\cos^2(\Phi_i)\right] = [\frac{1}{2} + \frac{2^b}{2\pi} \sin(\frac{\pi}{2^b}) \cos(\frac{\pi}{2^b})] = \frac{1+p}{2}$. Next, we have

$$\begin{aligned}
\mathbb{E}[C^2] &= \mathbb{E}\left[\left(2\alpha^2\sum_{i=1}^{N-1}\sum_{k=i+1}^{N}|[\mathbf{h}^{SR}]_i||[\mathbf{h}^{RD}]_i||[\mathbf{h}^{SR}]_k||[\mathbf{h}^{RD}]_k|\cos(\Phi_i-\Phi_k)\right)^2\right] \\
&= 4\alpha^4\sum_{i=1}^{N-1}\sum_{k=i+1}^{N}\left(\mathbb{E}\left[|[\mathbf{h}^{SR}]_i|^2\right]\right)^2\left(\mathbb{E}\left[|[\mathbf{h}^{RD}]_i|^2\right]\right)^2\mathbb{E}\left[\cos^2(\Phi_i-\Phi_k))\right] \\
&+ 4\alpha^4\sum_{j=1}^{N}\sum_{\substack{i=1\\ i\neq j\neq k\neq l}}^{N-1}\sum_{k=i+1}^{N}\sum_{l=j+1}^{N}\left(\mathbb{E}\left[|\left[\mathbf{h}^{SR}\right]_i|\right]\right)^4\left(\mathbb{E}\left[|\left[\mathbf{h}^{RD}\right]_i|\right]\right)^4\mathbb{E}^2\left[\cos\left(\Phi_i-\Phi_k\right)\right] \\
&+ 4\alpha^4\sum_{j=1}^{N}\sum_{\substack{i=1\\ j=i\neq k\neq l}}^{N-1}\sum_{k=i+1}^{N}\sum_{l=j+1}^{N}\Big[\mathbb{E}\left[|[\mathbf{h}^{SR}]_k|\right]\mathbb{E}\left[|[\mathbf{h}^{RD}]_k|\right]\mathbb{E}\left[|[\mathbf{h}^{SR}]_l|\right]\mathbb{E}\left[|[\mathbf{h}^{RD}]_l|\right] \\
&\qquad\qquad \mathbb{E}\left[|[\mathbf{h}^{SR}]_i|^2\right]\mathbb{E}\left[|[\mathbf{h}^{RD}]_i|^2\right]\mathbb{E}\left[\cos(\Phi_i-\Phi_k)\cos(\Phi_i-\Phi_l)\right]\Big].
\end{aligned} \tag{A.42}$$

Using $\mathbb{E}\left[\cos^2(\Phi_i-\Phi_k)\right] = \frac{1}{2}+\frac{1}{2}\left(\frac{\sin\left(2\frac{\pi}{2^b}\right)}{2\frac{\pi}{2^b}}\right)^2 = \frac{1+p^2}{2}$ and $\mathbb{E}\left[\cos\left(\Phi_i-\Phi_k\right)\cos(\Phi_i-\Phi_l)\right] = \frac{1}{2}s^2+\frac{1}{2}ps^2$, (A.42) can now be written as

$$\begin{aligned}
\mathbb{E}\left[C^2\right] &= N(N-1)\alpha^4\Big[(N-2)m_2^{sr}m_2^{rd}s^2\left(1+p\right)(m_1^{sr})^2(m_1^{rd})^2 + (m_2^{sr})^2(m_2^{rd})^2(1+p^2) \\
&\quad + s^4(N-2)(N-3)(m_1^{sr})^4(m_1^{rd})^4\Big].
\end{aligned} \tag{A.43}$$

Next, we derive the expectation of RV's AB, BC, and AC,

$$\mathbb{E}[AB] = \mathbb{E}\left[\left(|h^{SD}|^2+\alpha^2\sum_{i=1}^{N}|[\mathbf{h}^{SR}]_i|^2|[\mathbf{h}^{RD}]_i|^2\right)\times\left(2\alpha|h^{SD}|\sum_{i=1}^{N}|[\mathbf{h}^{SR}]_i||[\mathbf{h}^{RD}]_i|\cos(\Phi_i)\right)\right]. \tag{A.44}$$

As all the channel coefficients are assumed to be independent of each other, we can rewrite the above equation as (A.45).

$$\begin{aligned}
\mathbb{E}\left[AB\right] =& 2\alpha\mathbb{E}\left[|h^{SD}|^3\right]\sum_{i=1}^{N}\mathbb{E}\left[|[\mathbf{h}^{SR}]_i|\right]\mathbb{E}\left[|[\mathbf{h}^{RD}]_i|\right]\mathbb{E}\left[\cos(\Phi_i)\right] \\
&+ 4\alpha^3\mathbb{E}\left[|h^{SD}|\right]\sum_{j=1}^{N-1}\sum_{i=j+1}^{N}\mathbb{E}\left[|[\mathbf{h}^{SR}]_i|^2\right]\mathbb{E}\left[|[\mathbf{h}^{RD}]_i|^2\right]\mathbb{E}\left[|[\mathbf{h}^{SR}]_i|\right]\mathbb{E}\left[|[\mathbf{h}^{RD}]_i|\right]\mathbb{E}\left[\cos(\Phi_i)\right] \\
&+ 2\alpha^3\mathbb{E}\left[|h^{SD}|\right]\sum_{i=1}^{N}\mathbb{E}\left[|[\mathbf{h}^{SR}]_i|^3\right]\mathbb{E}\left[|[\mathbf{h}^{RD}]_i|^3\right]\mathbb{E}\left[\cos(\Phi_i)\right]).
\end{aligned} \tag{A.45}$$

Using $\mathbb{E}[|h^{ab}|^3] = m_3^{ab}$ where $a, b \in \{\mathbf{S}, \mathbf{R}, \mathbf{D}\}$, we have

$$\mathbb{E}[AB] = 2N\alpha m_3^{sd} m_1^{sr} m_1^{rd} s + 2\alpha^3 N m_1^{sd} m_3^{sr} m_3^{rd} s + 4\alpha^3 m_1^{sd} m_1^{sr} m_1^{rd} m_2^{sr} m_2^{rd} \frac{N(N-1)}{2} s. \tag{A.46}$$

Next we consider the expectation of the term BC,

$$\mathbb{E}[BC] = \mathbb{E}\left[2\alpha|h_{SD}| \sum_{i=1}^{N} |[\mathbf{h}_{SR}]_i||[\mathbf{h}_{RD}]_i| \cos(\Phi_i) \times 2\alpha^2 \sum_{i=1}^{N-1} \sum_{k=i+1}^{N} |[\mathbf{h}_{SR}]_i||[\mathbf{h}_{RD}]_i||[\mathbf{h}_{SR}]_k||[\mathbf{h}_{RD}]_k|(\cos(\Phi_i - \Phi_k))\right]. \tag{A.47}$$

As all the channel coefficients are assumed to be independent of each other, we can write the above equation as

$$\mathbb{E}[BC] = 4\alpha^3 m_1^{sd} \left[m_1^{sr}\right]^3 \left[m_1^{rd}\right]^3 \frac{N(N-1)(N-2)s^3}{2} \tag{A.48}$$

$$+ 2 * 4\alpha^3 m_1^{sd} m_2^{sr} m_2^{rd} m_1^{sr} m_1^{rd} \frac{N(N-1)}{2} s \frac{1+p}{2}. \tag{A.49}$$

Finally, we evaluate the expectation of the last term AC,

$$\mathbb{E}[AC] = \mathbb{E}\left[\left(|h^{SD}|^2 + \alpha^2 \sum_{i=1}^{N} |[\mathbf{h}^{SR}]_i|^2 |[\mathbf{h}^{RD}]_i|^2\right) \times \left(2\alpha^2 \sum_{i=1}^{N-1} \sum_{k=i+1}^{N} |[\mathbf{h}^{SR}]_i||[\mathbf{h}^{RD}]_i||[\mathbf{h}^{SR}]_k||[\mathbf{h}^{RD}]_k| \cos(\Phi_i - \Phi_k)\right)\right]. \tag{A.50}$$

As all the channel coefficients are assumed to be independent of each other, we can rewrite the above equation as

$$\begin{aligned}\mathbb{E}[AC] =& \mathbb{E}[|h^{SD}|^2]\mathbb{E}[C] \\ &+ 2\alpha^4 \sum_{i=1}^{N-1} \sum_{k=i+1}^{N} \mathbb{E}[|[\mathbf{h}^{SR}]_j|^3]\mathbb{E}[|[\mathbf{h}^{RD}]_j|^3]\mathbb{E}[|[\mathbf{h}^{SR}]_j|]\mathbb{E}[|[\mathbf{h}^{RD}]_j|]\mathbb{E}[\cos(\Phi_i - \Phi_k)] \\ &+ 4\alpha^4 \sum_{j=1}^{N} \sum_{\substack{i=1 \\ i\neq j\neq k}}^{N-1} \sum_{k=i+1}^{N} \mathbb{E}[|[\mathbf{h}^{SR}]_j|^2]\mathbb{E}[|[\mathbf{h}^{RD}]_j|^2]\mathbb{E}[|[\mathbf{h}^{SR}]_j|]^2\mathbb{E}[|[\mathbf{h}^{RD}]_j|]^2\mathbb{E}[\cos(\Phi_i - \Phi_k)].\end{aligned} \tag{A.51}$$

Substituting for the expectations, we get

$$\begin{aligned}\mathbb{E}[AC] =& m_2^{sd}\mathbb{E}[C] + 2\alpha^4 m_3^{sr} m_3^{rd} m_1^{sr} m_1^{rd} \frac{N(N-1)}{2} s^2 \\ &+ 4\alpha^4 (m_1^{sr})^2 (m_1^{rd})^2 m_2^{sr} m_2^{rd} \frac{N(N-1)(N-2)}{2} s^2. \end{aligned} \tag{A.52}$$

Thus, the first and second moments are obtained by substituting moments in

$$\mathbb{E}\left[\gamma_{IRS}\right] = \gamma_s \left(m_2^{sd} + N\alpha^2 m_2^{sr} m_2^{rd} + 2Ns\ \alpha m_1^{sd} m_1^{sr} m_1^{rd} + 2\alpha^2 (m_1^{sr})^2 (m_1^{rd})^2 \frac{N(N-1)}{2} s^2 \right). \tag{A.53}$$

$$\begin{aligned}\mathbb{E}\left[{\gamma_{IRS}}^2\right] = \gamma_s^2 \Bigg(& m_4^{sd} + 2\alpha^2 N m_2^{sr} m_2^{rd} m_2^{sd} + N\alpha^4 m_4^{sr} m_4^{rd} + 2\alpha^4 \frac{N(N-1)}{2} (m_2^{sr})^2 (m_2^{rd})^2 \\ & + 4\alpha^2 m_2^{sd} \left[N m_2^{sr} m_2^{rd} [\frac{1+p}{2}] + 2s^2 \frac{N(N-1)}{2} (m_2^{sr})^2 (m_2^{rd})^2 \right] \\ & + N(N-1)\alpha^4 \left[(N-2) m_2^{sr} m_2^{rd} s^2 \left(1+p\right) (m_1^{sr})^2 (m_1^{rd})^2 \right. \\ & \left. + (m_2^{sr})^2 (m_2^{rd})^2 (1+p^2) + s^4 (N-2)(N-3) (m_1^{sr})^4 (m_1^{rd})^4 \right] \\ & + 2 \left[2N\alpha m_3^{sd} m_1^{sr} m_1^{rd} s + 2\alpha^3 N m_1^{sd} m_3^{sr} m_3^{rd} s + 4\alpha^3 m_1^{sd} m_1^{sr} m_1^{rd} m_2^{sr} m_2^{rd} \frac{N(N-1)}{2} s \right] \\ & + 2 \frac{N(N-1)}{2} \left[4\alpha^3 m_1^{sd} \left[m_1^{sr}\right]^3 \left[m_1^{rd}\right]^3 (N-2) s^3 + 2 * 4\alpha^3 m_1^{sd} m_2^{sr} m_2^{rd} m_1^{sr} m_1^{rd} s \frac{1+p}{2} \right] \\ & + 4\alpha^2 \frac{N(N-1)}{2} s^2 m_1^{sr} m_1^{rd} \left[m_2^{sd} m_1^{sr} m_1^{rd} + \alpha^2 \left[m_3^{sr} m_3^{rd} + 2 m_1^{sr} m_1^{rd} m_2^{sr} m_2^{rd} (N-2) \right] \right] \Bigg). \end{aligned} \tag{A.54}$$

A.5 Proof for Theorem 4

When Source to Destination link is in outage, the resultant SNR at node D is given by

$$\gamma_{IRS} = \gamma_s |(|h^{SD}| + \alpha \sum_{i=1}^{N} |[\mathbf{h}^{SR}]_i| |[\mathbf{h}^{RD}]_i|)|^2. \tag{A.55}$$

The CDF of γ_{IRS} can be evaluated as

$$F_{\gamma_{IRS}}(\gamma) = \mathbb{P}\left(\gamma_s |(|h^{SD}| + \alpha \sum_{i=1}^{N} |[\mathbf{h}^{SR}]_i| |[\mathbf{h}^{RD}]_i|)|^2 \leq \gamma \right). \tag{A.56}$$

$$F_{\gamma_{IRS}}(\gamma) = \mathbb{P}\left(\alpha^2|(\frac{\sqrt{\gamma_s}}{\alpha}|h^{SD}| + \sum_{i=1}^{N}\sqrt{\gamma_s}|[\mathbf{h}^{SR}]_i||[\mathbf{h}^{RD}]_i)|^2 \leq \gamma\right). \tag{A.57}$$

$$F_{\gamma_{IRS}}(\gamma) = \mathbb{P}\left(|(\frac{\sqrt{\gamma_s}}{\alpha}|h^{SD}| + \sum_{i=1}^{N}\sqrt{\gamma_s}|[\mathbf{h}^{SR}]_i||[\mathbf{h}^{RD}]_i)| \leq \frac{\sqrt{\gamma}}{\alpha}\right). \tag{A.58}$$

Let $Z = Y + \sum_{i=1}^{N} X_i$, where $Y = \frac{\sqrt{\gamma_s}}{\alpha}|h^{SD}|$, $X = \left[\sqrt{\gamma_s}|[\mathbf{h}^{SR}]_1||[\mathbf{h}^{RD}]_1, \ldots, \sqrt{\gamma_s}|[\mathbf{h}^{SR}]_N||[\mathbf{h}^{RD}]_N\right]^T = [X_1, \ldots, X_N]^T$, is a multivariate vector with i.i.d. entries.

The p.d.f. of Y is as follows

$$f_Y(y) = \frac{\alpha^2}{\gamma_s\sigma_{sd}^2} y e^{-\frac{\alpha^2}{2\gamma_s\sigma_{sd}^2}y^2} \tag{A.59}$$

The p.d.f. of X_i's

$$f_{X_i}(x_i) = \frac{4d_{sr}^{\beta}d_{rd}^{\beta}}{\gamma_s} x_i \mathrm{K}_0\left[\frac{2x_i}{\sqrt{\gamma_s}d_{sr}^{-\beta/2}d_{rd}^{-\beta/2}}\right] \tag{A.60}$$

Assuming $a^2 := \frac{4d_{sr}^{\beta}d_{rd}^{\beta}}{\gamma_s}$, $b^2 = \frac{\gamma_s\sigma_{sd}^2}{2\alpha^2}$, and using inequality $\mathrm{K}_0(ax) \leq \frac{\sqrt{\pi}e^{-ax}}{\sqrt{2ax}}$, above equation can be written as

$$\begin{aligned} f_{X_i}(x_i) =& a^2 x_i \mathbf{K}_0(ax_i) \\ \leq& a^2 x_i \frac{\sqrt{\pi}\exp(-ax_i)}{\sqrt{2ax_i}} \\ \leq& \sqrt{\frac{\pi x_i}{2}} a^{\frac{3}{2}} \exp(-ax_i). \end{aligned} \tag{A.61}$$

$$f_Y(y) = \frac{y}{\sigma^2} e^{-\frac{y^2}{2\sigma^2}} \tag{A.62}$$

Laplace Transforms of RV's X_i,Y are given by

$$\begin{aligned} \mathbb{L}(f_Y(y)) = \mathbb{L}(\frac{y}{\sigma^2}e^{-\frac{y^2}{2\sigma^2}}) =& \frac{1}{2}\left[2 - e^{\frac{s^2\sigma^2}{2}}\sqrt{2\pi}s\sigma\mathrm{erfc}[\frac{s\sigma}{\sqrt{2}}]\right] \\ =& 1 - e^{s^2b^2}\sqrt{\pi}sb\ \mathrm{erfc}[sb] \end{aligned} \tag{A.63}$$

$$\mathbb{L}[f_{X_i}(x_i)] \leq \sqrt{\frac{\pi}{2}} a^{\frac{3}{2}}\ \mathbb{L}[x_i^{\frac{1}{2}}\exp(-ax_i)]. \tag{A.64}$$

We know that $\mathbb{L}[t^{\frac{1}{2}}] = \frac{\sqrt{\pi}}{2s^{\frac{3}{2}}}$, and $\mathbb{L}[e^{-at}f(t)] = F(s+a)$, we can write above

equation as

$$\begin{aligned}\mathbb{L}[f_{X_i}(x_i)] \leq & \sqrt{\frac{\pi}{2}} a^{\frac{3}{2}} \frac{\sqrt{\pi}}{2(s+a)^{\frac{3}{2}}} \\ \leq & \frac{\pi a^{\frac{3}{2}}}{2^{\frac{3}{2}}} \frac{1}{(s+a)^{\frac{3}{2}}}. \end{aligned} \tag{A.65}$$

Since all X_i follow the same PDF given by A.61, the PDF of Z can be found from

$$f_Z(z) = \mathbb{L}^{-1}(\mathbb{L}f_Y(y)[\mathbb{L}f_{X_i}(x_i)]^N) \tag{A.66}$$

On substituting Laplace Transform's, we now find PDF of upper bound given by

$$f_Z(z) \leq \mathbb{L}^{-1}\left(\left[1 - e^{s^2b^2}\sqrt{\pi} sb \text{ erfc}[sb]\right]\left[\frac{\pi a^{\frac{3}{2}}}{2^{\frac{3}{2}}(s+a)^{\frac{3}{2}}}\right]^N\right) \tag{A.67}$$

Since inverse laplace is linear function rearrangement of above equation gives

$$f_Z(z) \leq \frac{\pi^N a^{\frac{3N}{2}}}{2^{\frac{3N}{2}}}\left[\mathbb{L}^{-1}\left[\frac{1}{(s+a)^{\frac{3N}{2}}}\right] - \sqrt{\pi} b \mathbb{L}^{-1}\left[s\frac{e^{s^2b^2}\text{erfc}[sb]}{(s+a)^{\frac{3N}{2}}}\right]\right] \tag{A.68}$$

Substituting for Inverse laplace transform results in

$$\begin{aligned} f_Z(z) \leq & \frac{\pi^N a^{\frac{3N}{2}}}{2^{\frac{3N}{2}}}\left[\frac{e^{-at} z^{\frac{3N}{2}-1}}{\Gamma(\frac{3N}{2})}\right] \\ & - \frac{\pi^N a^{\frac{3N}{2}}}{2^{\frac{3N}{2}}}\sqrt{\pi} b\left[\frac{2^{\frac{3N}{2}-1}(\frac{1}{b^2})^{-\frac{3N}{4}} e^{-\frac{z^2}{4b^2}}}{\Gamma[\frac{3N}{2}] b\sqrt{\Pi}}\left[(\frac{-z}{2b^2})\left[\Gamma[\frac{3N}{4}]F_1[\frac{3N}{4}, \frac{1}{2}, \frac{(-2ab^2+z)^2}{4b^2}]\right.\right.\right. \\ & \left.\left.\left. + \sqrt{\frac{1}{b^2}}(-2ab^2+z)\Gamma[\frac{1}{2}+\frac{3N}{4}]F_1[\frac{2+3N}{4}, \frac{3}{2}, \frac{(-2ab^2+z)^2}{4b^2}]\right]\right] \\ & + \frac{2^{-1+\frac{3N}{2}}(\frac{1}{b^2})^{-\frac{3N}{4}} e^{-\frac{z^2}{4b^2}}}{\Gamma[\frac{3N}{2}] b\sqrt{\Pi}}\left[\Gamma[\frac{3N}{4}]\frac{3N(-2ab^2+z)}{4b^2}F_1[1+\frac{3N}{4}, \frac{3}{2}, \frac{(-2ab^2+z)^2}{4b^2}]\right. \\ & + \sqrt{\frac{1}{b^2}}\Gamma[\frac{1}{2}+\frac{3N}{4}]F_1[\frac{2+3N}{4}, \frac{3}{2}, \frac{(-2ab^2+z)^2}{4b^2}] \\ & \left. + \sqrt{\frac{1}{b^2}}\frac{(-2ab^2+z)^2}{12b^2}\Gamma[\frac{1}{2}+\frac{3N}{4}]F_1[\frac{6+3N}{4}, \frac{5}{2}, \frac{(-2ab^2+z)^2}{4b^2}]\right] \end{aligned} \tag{A.69}$$

We can now find the bound to outage probability by

$$P_{Outage}(t) = \int_0^t f_Z(z)dz \tag{A.70}$$

Finally, the upper bound to OP for an IRS system with SD link is given by

$$\begin{aligned}
P_{outage} \leq & \int_0^t \frac{\pi^N a^{\frac{3N}{2}}}{2^{\frac{3N}{2}}} \left[\frac{e^{-at} z^{\frac{3N}{2}-1}}{\Gamma(\frac{3N}{2})}\right] dz \\
& - \frac{\pi^N a^{\frac{3N}{2}}}{2^{\frac{3N}{2}}} \sqrt{\pi} b \int_0^t \left[\frac{2^{\frac{3N}{2}-1} (\frac{1}{b^2})^{-\frac{3N}{4}} e^{-\frac{z^2}{4b^2}}}{\Gamma[\frac{3N}{2}] b\sqrt{\Pi}} \left[(\frac{-z}{2b^2}) \left[\Gamma[\frac{3N}{4}] {}_1F_1[\frac{3N}{4}, \frac{1}{2}, \frac{(-2ab^2+z)^2}{4b^2}]\right.\right.\right. \\
& \left.\left.\left. + \sqrt{\frac{1}{b^2}}(-2ab^2+z)\Gamma[\frac{1}{2}+\frac{3N}{4}] {}_1F_1[\frac{2+3N}{4}, \frac{3}{2}, \frac{(-2ab^2+z)^2}{4b^2}]\right]\right] \\
& + \frac{2^{-1+\frac{3N}{2}} (\frac{1}{b^2})^{-\frac{3N}{4}} e^{-\frac{z^2}{4b^2}}}{\Gamma[\frac{3N}{2}] b\sqrt{\Pi}} \left[\Gamma[\frac{3N}{4}] \frac{3N(-2ab^2+z)}{4b^2} {}_1F_1[1+\frac{3N}{4}, \frac{3}{2}, \frac{(-2ab^2+z)^2}{4b^2}]\right. \\
& + \sqrt{\frac{1}{b^2}}\Gamma[\frac{1}{2}+\frac{3N}{4}] {}_1F_1[\frac{2+3N}{4}, \frac{3}{2}, \frac{(-2ab^2+z)^2}{4b^2}] \\
& \left. + \sqrt{\frac{1}{b^2}} \frac{(-2ab^2+z)^2}{12b^2} \Gamma[\frac{1}{2}+\frac{3N}{4}] {}_1F_1[\frac{6+3N}{4}, \frac{5}{2}, \frac{(-2ab^2+z)^2}{4b^2}]\right] dz,
\end{aligned} \tag{A.71}$$

Here, ${}_1F_1(\cdot,\cdot,\cdot)$ is the confluent hypergeometric function of the first kind [35].

A.6 Proof for Theorem 5

When Source to Destination link is in outage, the resultant SNR at node D is given by

$$\gamma_{IRS} = \gamma_s |\alpha \sum_{i=1}^{N} |[\mathbf{h}^{SR}]_i| |[\mathbf{h}^{RD}]_i||^2. \tag{A.72}$$

The CDF of γ_{IRS} can now be evaluated as

$$F_{\gamma_{IRS}}(\gamma) = \mathbb{P}\left(\gamma_s |\alpha \sum_{i=1}^{N} |[\mathbf{h}^{SR}]_i| |[\mathbf{h}^{RD}]_i||^2 \leq \gamma\right). \tag{A.73}$$

$$F_{\gamma_{IRS}}(\gamma) = \mathbb{P}\left(|\sum_{i=1}^{N} \sqrt{\gamma_s} |[\mathbf{h}^{SR}]_i| |[\mathbf{h}^{RD}]_i| \leq \frac{\sqrt{\gamma}}{\alpha}\right). \tag{A.74}$$

Let $Z = \sum_{i=1}^{N} X_i$, where $X = \left[\sqrt{\gamma_s}|[\mathbf{h}^{SR}]_1||[\mathbf{h}^{RD}]_1, \ldots, \sqrt{\gamma_s}|[\mathbf{h}^{SR}]_N||[\mathbf{h}^{RD}]_N\right]^T = [X_1, \ldots, X_N]^T$, is a multivariate vector with i.i.d. entries whose PDF is given as follows:

$$f_{X_i}(x_i) = \frac{4d_{sr}^{\beta} d_{rd}^{\beta}}{\gamma_s} x_i \mathrm{K}_0 \left[\frac{2x_i}{\sqrt{\gamma_s} d_{sr}^{-\beta/2} d_{rd}^{-\beta/2}}\right] \tag{A.75}$$

Assuming $a^2 := \frac{4d_{sr}^{\beta} d_{rd}^{\beta}}{\gamma_s}$, and using inequality $\mathrm{K}_0(ax) \leq \frac{\sqrt{\pi} e^{-ax}}{\sqrt{2ax}}$, above equation can be written as

$$\begin{aligned} f_{X_i}(x_i) =& a^2 x_i \mathbf{K}_0 (a x_i) \\ \leq& a^2 x_i \frac{\sqrt{\pi} \exp(-a x_i)}{\sqrt{2a x_i}} \\ =& \sqrt{\frac{\pi x_i}{2}} a^{\frac{3}{2}} \exp(-a x_i). \end{aligned} \tag{A.76}$$

Applying Laplace Transform

$$\mathbb{L}[f_{X_i}(x_i)] \leq \sqrt{\frac{\pi}{2}} a^{\frac{3}{2}} \, \mathbb{L}[x_i^{\frac{1}{2}} \exp(-a x_i)]. \tag{A.77}$$

If $\mathbb{L}[f(t)] = F(s)$, then $\mathbb{L}[e^{-at} f(t)] = F(s+a)$, $\mathbb{L}[t^{\frac{1}{2}}] = \frac{\sqrt{\pi}}{2s^{\frac{3}{2}}}$, we can write above equation as

$$\begin{aligned} \mathbb{L}[f_{X_i}(x_i)] \leq& \sqrt{\frac{\pi}{2}} a^{\frac{3}{2}} \, \frac{\sqrt{\pi}}{2(s+a)^{\frac{3}{2}}} \\ =& \frac{\pi a^{\frac{3}{2}}}{2^{\frac{3}{2}}} \frac{1}{(s+a)^{\frac{3}{2}}}. \end{aligned} \tag{A.78}$$

Since all X_i follow the same PDF, the PDF of Z can be found from

$$f_Z(z) = \mathbb{L}^{-1}[\mathbb{L}^N f_{X_i}(x_i)] \tag{A.79}$$

$$\begin{aligned} f_Z(z) \leq& \mathbb{L}^{-1} \left[\frac{\pi^N a^{\frac{3N}{2}}}{2^{\frac{3N}{2}}} \frac{1}{(s+a)^{\frac{3N}{2}}}\right] \\ \leq& \frac{\pi^N a^{\frac{3N}{2}}}{2^{\frac{3N}{2}}} \mathbb{L}^{-1}\left[\frac{1}{(s+a)^{\frac{3N}{2}}}\right] \end{aligned} \tag{A.80}$$

Using $\mathbb{L}^{-1}[\frac{\Gamma[n+1]}{s^{n+1}}] = t^n$, and $\mathbb{L}^{-1}[F(s+a)] = e^{-at}f(t)$, we get

$$f_Z(z) \leq \frac{\pi^N a^{\frac{3N}{2}}}{2^{\frac{3N}{2}}} \frac{e^{-at} z^{\frac{3N}{2}-1}}{\Gamma(\frac{3N}{2})} \tag{A.81}$$

We know that outage expression is given by

$$P_{Outage}(t) = \int_0^t f_Z(z)dz \tag{A.82}$$

$$P_{Outage}(t) \leq \frac{\pi^N}{2^{\frac{3N}{2}}} \frac{\gamma(\frac{3N}{2}, at)}{\Gamma(\frac{3N}{2})} \tag{A.83}$$

A.7 Proof for Theorem 6

The expression for P_{outage} (for the case without phase error) is given by

$$P_{outage} = \mathbb{P}\left(\left(|h_{sd}| + \sum_{i=1}^{N} |[\mathbf{h}_{SR}]_i||[\mathbf{h}_{RD}]_i|\right)^2 \leq \gamma\right). \tag{A.84}$$

Let $\mathbf{m}_{SR} := [\sqrt{|h_{SD}|}\,|[\mathbf{h}_{SR}]_1|\ \cdots\ ,\ |[\mathbf{h}_{SR}]_N|]$ and $\mathbf{m}_{RD} := [\sqrt{|h_{SD}|}\,|[\mathbf{h}_{RD}]_1|\ \cdots\ ,\ |[\mathbf{h}_{RD}]_N|]$. Thus, we have

$$P_{outage} = \mathbb{P}\left(\langle \mathbf{m}_{SR}, \mathbf{m}_{RD}\rangle^2 \leq \gamma\right) \leq \mathbb{P}\left(\langle \mathbf{m}_{SR}, \mathbf{m}_{SR}\rangle \,.\, \langle \mathbf{m}_{RD}, \mathbf{m}_{RD}\rangle \leq \gamma\right). \tag{A.85}$$

Note that $\tilde{m}_{SR} := \langle \mathbf{m}_{SR}, \mathbf{m}_{SR}\rangle = |h_{SD}| + \sum_{i=1}^{N} |[\mathbf{h}_{SR}]_i|^2$. We have $|[h_{RD}]_i|^2 \sim \text{Exp}(\frac{1}{2\sigma_{sr}^2})$. Then, $\tilde{h}_{SR} := \sum_{i=1}^{N} |[\mathbf{h}_{SR}]_i|^2 \sim \text{Gamma}\,(N, 2\sigma_{sr}^2)$. Similarly, let $\tilde{m}_{RD} := \langle \mathbf{m}_{RD}, \mathbf{m}_{RD}\rangle$. To characterise the probability of outage, we need to characterise the CDF of the RV $Z = \tilde{m}_{SR} \times \tilde{m}_{RD} = (|h_{SD}| + \tilde{h}_{SR}) \times (|h_{SD}| + \tilde{h}_{RD})$. Note that the RV Z is the product of two correlated RVs. In the following discussion we use the Jacobian method to characterise the distribution of Z. We briefly discuss the Jacobian method of transforming RVs in the next paragraph:

Consider an n-tuple random variable $(X_1, X_2, \ldots, X_n)$ whose joint density is given by

$f_{(X_1,X_2,\ldots,X_n)}\,(x_1, x_2, \ldots, x_n)$ and the corresponding transformations are given by

$Y_1 = g_1\,(X_1, X_2, \ldots, X_n)\,, Y_2 = g_2\,(X_1, X_2, \ldots, X_n)\,, \ldots, Y_n = g_n\,(X_1, X_2, \ldots, X_n)\,.$

Succinctly, we denote this as a vector transformation $Y = g(X)$, where $g : \mathbb{R}^n \to \mathbb{R}^n$. We assume that the transformation g is invertible, and continuously differentiable. Under this assumption, the joint density of $f_{Y_1,Y_2,\ldots,Y_n}(Y_1, Y_2, \ldots, Y_n)$ is given by

$$f_{Y_1,Y_2,\ldots,Y_n}(y_1, y_2, \ldots, y_n) = f_{(X_1,X_2,\ldots,X_n)}\left(g_1^{-1}(y)\right)|J(y)|$$

where $|J(y)|$ is the Jacobian matrix, given by

$$J(y) = \begin{vmatrix} \frac{\partial x_1}{\partial y_1} & \frac{\partial x_2}{\partial y_1} & . & . & . & \frac{\partial x_n}{\partial y_1} \\ \frac{\partial x_1}{\partial y_2} & \frac{\partial x_2}{\partial y_2} & . & . & . & \frac{\partial x_n}{\partial y_2} \\ . & . & & & & . \\ . & . & & \ddots & & . \\ . & . & & & & . \\ \frac{\partial x_1}{\partial y_n} & \frac{\partial x_2}{\partial y_n} & . & . & . & \frac{\partial x_n}{\partial y_n} \end{vmatrix}.$$

Here, we have $X_1 = |h_{SD}|, X_2 = \tilde{h}_{SR}$ and $X_3 = \tilde{h}_{RD}$. Similarly, let $Y_1 = (X_1 + X_2)\times(X_1+X_3)$, $Y_2 = X_2$ and $Y_3 = X_3$. Note that $X_1 = \frac{1}{2}\left(-y_2 - y_3 \pm \sqrt{4y_1 + y_2^2 - 2y_2y_3 + y_3^2}\right)$, $X_2 = Y_2$ and $X_3 = Y_3$. Since, we know that $X_i > 0 \ \forall \ i$, we choose $X_1 = \frac{1}{2}\left(-y_2 - y_3 + \sqrt{4y_1 + y_2^2 - 2y_2y_3 + y_3^2}\right)$. Since the RVs X_1, X_2, X_3 are independent, their joint distribution $f_{(X_1,X_2,X_3)}$ is given by

$$f_{(X_1,X_2,X_3)} = \frac{x_1}{\sigma_{sd}^2} e^{-x_1^2/\left(2\sigma_{sd}^2\right)} \times \frac{1}{\Gamma(N)(2\sigma_{sr}^2)^N} x_2^{N-1} e^{-\frac{x_2}{(2\sigma_{sr}^2)}} \times \frac{1}{\Gamma(N)(2\sigma_{rd}^2)^N} x_3^{N-1} e^{-\frac{x_3}{(2\sigma_{rd}^2)}}. \tag{A.86}$$

The corresponding Jacobian is given by

$$J(y) = \begin{vmatrix} \frac{\partial x_1}{\partial y_1} & 0 & 0 \\ \frac{\partial x_1}{\partial y_2} & 1 & 0 \\ \frac{\partial x_1}{\partial y_3} & 0 & 1 \end{vmatrix} = \frac{\partial x_1}{\partial y_1} = \left(4y_1 + (y_2 - y_3)^2\right)^{\frac{-1}{2}}.$$

Thus, we have

$$\begin{aligned} f_{Y_1,Y_2,Y_3}(y_1, y_2, y_3) = \frac{x_1}{\sigma_{sd}^2} e^{-x_1^2/\left(2\sigma_{sd}^2\right)} \times \frac{1}{\Gamma(N)(2\sigma_{sr}^2)^N} y_2^{N-1} e^{-\frac{y_2}{(2\sigma_{sr}^2)}} \times \frac{1}{\Gamma(N)(2\sigma_{rd}^2)^N} y_3^{N-1} e^{-\frac{y_3}{(2\sigma_{rd}^2)}} \\ \times \ \left(4y_1 + (y_2 - y_3)^2\right)^{\frac{-1}{2}}, \end{aligned} \tag{A.87}$$

where $x_1 = \frac{1}{2}\left(-y_2 - y_3 + \sqrt{4y_1 + y_2^2 - 2y_2y_3 + y_3^2}\right)$. Now, to derive the marginal CDF of the RV Y_1 we can integrate (A.87) over the support of Y_2 and Y_3. Note that $X_1 > 0$ will require the following condition:

$$\frac{1}{2}\left(-y_2 - y_3 \pm \sqrt{4y_1 + y_2^2 - 2y_2y_3 + y_3^2}\right) > 0, \tag{A.88}$$

$$\text{i.e } \sqrt{4y_1 + y_2^2 - 2y_2y_3 + y_3^2} > y_2 + y_3, \tag{A.89}$$

$$\text{i.e } y_1 > y_2y_3 \tag{A.90}$$

$$\text{i.e } y_2 < \frac{y_1}{y_3}. \tag{A.91}$$

Thus, we have

$$f_{Y_1}(y_1) = \int_0^{\infty}\int_0^{\frac{y_1}{y_3}} f_{Y_1,Y_2,Y_3}(y_1, y_2, y_3)\ dy_2\ dy_3. \tag{A.92}$$

Hence, CDF of Y_1 is given by

$$F_{Y_1}(t) = \int_0^{t}\int_0^{\infty}\int_0^{\frac{y_1}{y_3}} f_{Y_1,Y_2,Y_3}(y_1, y_2, y_3)\ dy_2\ dy_3\ dy_1. \tag{A.93}$$

where

$$f_{Y_1,Y_2,Y_3}(y_1, y_2, y_3) = \frac{\frac{1}{2}\left(-y_2 - y_3 + \sqrt{4y_1 + y_2^2 - 2y_2y_3 + y_3^2}\right)}{\sigma_{sd}^2} e^{-\frac{(\frac{1}{2}\left(-y_2 - y_3 + \sqrt{4y_1 + y_2^2 - 2y_2y_3 + y_3^2}\right))^2}{\left(2\sigma_{sd}^2\right)}}$$
$$\frac{1}{\Gamma(N)(2\sigma_{sr}^2)^N} y_2^{N-1} e^{-\frac{y_2}{(2\sigma_{sr}^2)}} \frac{1}{\Gamma(N)(2\sigma_{rd}^2)^N} y_3^{N-1} e^{-\frac{y_3}{(2\sigma_{rd}^2)}} \times \left(4y_1 + (y_2 - y_3)^2\right)^{\frac{-1}{2}}. \tag{A.94}$$

A.8 Proof for Theorem 7

The expression for P_{outage} (for the case without phase error) is given by

$$P_{outage} = \mathbb{P}\left(\left|\sum_{i=1}^{N} |[\mathbf{h}_{SR}]_i||[\mathbf{h}_{RD}]_i|\right|^2 \leq \gamma\right). \tag{A.95}$$

Using Cauchy-Scwartz inequality, we have

$$P_{outage} = \mathbb{P}\left(\gamma_s \langle \mathbf{h}_{SR}, \mathbf{h}_{RD}\rangle^2 \leq \gamma\right) \leq \mathbb{P}\left(\langle \mathbf{h}_{SR}, \mathbf{h}_{SR}\rangle . \langle \mathbf{h}_{RD}, \mathbf{h}_{RD}\rangle \leq \gamma\right). \tag{A.96}$$

$$P_{outage} \leq \mathbb{P}\left(\langle \mathbf{h}_{SR}, \mathbf{h}_{SR}\rangle \,.\, \langle \mathbf{h}_{RD}, \mathbf{h}_{RD}\rangle \leq \frac{\gamma}{\gamma_s}\right). \tag{A.97}$$

We have $|[\mathbf{h}_{SR}]_i|^2 \sim \text{Exp}(\frac{1}{2\sigma_{sr}^2})$. Then, $\tilde{h}_{SR} := \sum_{i=1}^{N} |[\mathbf{h}_{SR}]_i|^2 \sim \text{Gamma}\,(N, 2\sigma_{sr}^2)$. Similarly, $|[\mathbf{h}_{RD}]_i|^2 \sim \text{Exp}(\frac{1}{2\sigma_{rd}^2})$. Then, $\tilde{h}_{RD} := \sum_{i=1}^{N} |[\mathbf{h}_{RD}]_i|^2 \sim \text{Gamma}\,(N, 2\sigma_{rd}^2)$. To characterise the probability of outage, we need to characterise the CDF of the RV $Z = (\tilde{h}_{SR}) \times (\tilde{h}_{RD})$. Note that the RV Z is the product of two independent Gamma RVs whose PDF is given by

$$f_z(z) = \frac{2\left(\frac{z}{\sigma_{sr}\sigma_{rd}}\right)^N K_0\left(2\sqrt{\frac{z}{\sigma_{sr}\sigma_{rd}}}\right)}{z\Gamma^2[N]}. \tag{A.98}$$

We now found the CDF of Z using the integral

$$P_{outage} \leq \int_0^{\frac{\gamma}{\gamma_s}} f_z(z)dz. \tag{A.99}$$

Solving the above integral results in

$$P_{outage} \leq \frac{1}{N^2\Gamma^2[N]}\left(\frac{\gamma}{\gamma_s\sigma_{sr}\sigma_{rd}}\right)^N F\left[\{N,N\},\{1,1+N,1+N\},\frac{\gamma}{\gamma_s\sigma_{sr}\sigma_{rd}}\right] \tag{A.100}$$

$$- NF[\{N\},\{1,1+N\},\frac{\gamma}{\gamma_s\sigma_{sr}\sigma_{rd}}]\left(2\psi + Log[\frac{\gamma}{\gamma_s\sigma_{sr}\sigma_{rd}}]\right) \tag{A.101}$$

$$+ 2N^2\Gamma[N]F_r^{(\{1,0\},\{0,0,0\},\{0\})}\left[\{1,N\},\{1,1,1+N\},\{\frac{\gamma}{\gamma_s\sigma_{sr}\sigma_{rd}}\}\right] \tag{A.102}$$

$$. \tag{A.103}$$

Here, ${}_pF(\cdot,\cdot,\cdot)$ ${}_pF_r(\cdot,\cdot,\cdot)$ denotes the generalized and regularized confluent hypergeometric functions [35] and ψ is Euler gamma constant.

REFERENCES

[1] J. Zhang, E. Björnson, M. Matthaiou, D. W. K. Ng, H. Yang, and D. J. Love, "Prospective multiple antenna technologies for beyond 5g," *IEEE Journal on Selected Areas in Communications*, vol. 38, no. 8, pp. 1637–1660, 2020.

[2] F. Boccardi, R. W. Heath, A. Lozano, T. L. Marzetta, and P. Popovski, "Five disruptive technology directions for 5g," *IEEE Communications Magazine*, vol. 52, no. 2, pp. 74–80, 2014.

[3] E. Björnson, Ö. Özdogan, and E. G. Larsson, "Intelligent reflecting surface versus decode-and-forward: How large surfaces are needed to beat relaying?" *IEEE Wireless Communications Letters*, vol. 9, no. 2, pp. 244–248, 2019.

[4] N. Mensi, D. B. Rawat, and E. Balti, "Physical layer security for v2i communications: Reflecting surfaces vs. relaying," *arXiv preprint arXiv:2010.07216*, 2020.

[5] Q. Wu and R. Zhang, "Towards smart and reconfigurable environment: Intelligent reflecting surface aided wireless network," *IEEE Communications Magazine*, vol. 58, no. 1, pp. 106–112, 2019.

[6] E. Björnson., *Reconfigurable intelligent surfaces: Myths and realities*, (accessed March 18, 2020). [Online]. Available: https://www.youtube.com/watch?v=ysSf1K2NUu0&t=75s

[7] M. Di Renzo, A. Zappone, M. Debbah, M. S. Alouini, C. Yuen, J. de Rosny, and S. Tretyakov, "Smart radio environments empowered by reconfigurable intelligent surfaces: How it works, state of research, and the road ahead," *IEEE Journal on Selected Areas in Communications*, vol. 38, no. 11, pp. 2450–2525, 2020.

[8] E. Basar, M. Di Renzo, J. De Rosny, M. Debbah, M. Alouini, and R. Zhang, "Wireless communications through reconfigurable intelligent surfaces," *IEEE Access*, vol. 7, pp. 116 753–116 773, 2019.

[9] M. Di Renzo, K. Ntontin, J. Song, F. H. Danufane, X. Qian, F. Lazarakis, J. De Rosny, D. Phan-Huy, O. Simeone, R. Zhang, M. Debbah, G. Lerosey, M. Fink, S. Tretyakov, and S. Shamai, "Reconfigurable intelligent surfaces vs. relaying: Differences, similarities, and performance comparison," *IEEE Open Journal of the Communications Society*, vol. 1, pp. 798–807, 2020.

[10] Z. Wang, L. Liu, and S. Cui, "Intelligent reflecting surface assisted massive MIMO communications," in *2020 IEEE 21st International Workshop on Signal Processing Advances in Wireless Communications (SPAWC)*, 2020, pp. 1–5.

[11] X. Jia, J. Zhao, X. Zhou, and D. Niyato, "Intelligent reflecting surface-aided backscatter communications," in *GLOBECOM 2020 - 2020 IEEE Global Communications Conference*, 2020, pp. 1–6.

[12] S. Gopi, S. Kalyani, and L. Hanzo, "Intelligent reflecting surface assisted beam index-modulation for millimeter wave communication," *IEEE Transactions on Wireless Communications*, 2020.

[13] P. Wang, J. Fang, X. Yuan, Z. Chen, and H. Li, "Intelligent reflecting surface-assisted millimeter wave communications: Joint active and passive precoding design," *IEEE Transactions on Vehicular Technology*, 2020.

[14] A. S. d. Sena, D. Carrillo, F. Fang, P. H. J. Nardelli, D. B. d. Costa, U. S. Dias, Z. Ding, C. B. Papadias, and W. Saad, "What role do intelligent reflecting surfaces play in multi-antenna non-orthogonal multiple access?" *IEEE Wireless Communications*, vol. 27, no. 5, pp. 24–31, 2020.

[15] H. Du, J. Zhang, J. Cheng, and B. Ai, "Millimeter wave communications with reconfigurable intelligent surfaces: Performance analysis and optimization," *IEEE Transactions on Communications*, vol. 69, no. 4, pp. 2752–2768, 2021.

[16] Q. Tao, J. Wang, and C. Zhong, "Performance analysis of intelligent reflecting surface aided communication systems," *IEEE Communications Letters*, 2020.

[17] D. Kudathanthirige, D. Gunasinghe, and G. Amarasuriya, "Performance analysis of intelligent reflective surfaces for wireless communication," in *ICC 2020 - 2020 IEEE International Conference on Communications (ICC)*, 2020, pp. 1–6.

[18] P. Xu, G. Chen, G. Pan, and M. Di Renzo, "Ergodic secrecy rate of ris-assisted communication systems in the presence of discrete phase shifts and multiple eavesdroppers," *IEEE Wireless Communications Letters*, 2020.

[19] L. Yang and Y. Yuan, "Secrecy outage probability analysis for RIS-assisted NOMA systems," *Electronics Letters*, vol. 56, no. 23, pp. 1254–1256, 2020.

[20] Z. Tang, T. Hou, Y. Liu, J. Zhang, and L. Hanzo, "Physical layer security of intelligent reflective surface aided NOMA networks," *arXiv preprint arXiv:2011.03417*, 2020.

[21] D. Li, "Ergodic Capacity of Intelligent Reflecting Surface-Assisted Communication Systems with Phase Errors," *IEEE Communications Letters*, 2020.

[22] S. Atapattu, R. Fan, P. Dharmawansa, G. Wang, J. Evans, and T. A. Tsiftsis, "Reconfigurable intelligent surface assisted two–way communications: Performance analysis and optimization," *IEEE Transactions on Communications*, vol. 68, no. 10, pp. 6552–6567, 2020.

[23] F. A. De Figueiredo, M. S. Facina, R. C. Ferreira, Y. Ai, R. Ruby, Q.-V. Pham, and G. Fraidenraich, "Large intelligent surfaces with discrete set of phase-shifts communicating through double-Rayleigh fading channels," *IEEE Access*, vol. 9, pp. 20 768–20 787, 2021.

[24] T. Hou, Y. Liu, Z. Song, X. Sun, Y. Chen, and L. Hanzo, "MIMO assisted networks relying on large intelligent surfaces: A stochastic geometry model," *arXiv preprint arXiv:1910.00959*, 2019.

[25] Z. Cui, K. Guan, J. Zhang, and Z. Zhong, "SNR Coverage probability analysis of RIS-Aided Communication systems," *IEEE Transactions on Vehicular Technology*, pp. 1–1, 2021.

[26] S. Al-Ahmadi and H. Yanikomeroglu, "On the approximation of the generalized-k distribution by a gamma distribution for modeling composite fading channels," *IEEE Transactions on Wireless Communications*, vol. 9, no. 2, pp. 706–713, 2010.

[27] M. Srinivasan and S. Kalyani, "Secrecy capacity of $\kappa - \mu$ shadowed fading channels," *IEEE Communications Letters*, vol. 22, no. 8, pp. 1728–1731, 2018.

[28] T. Wang, G. Chen, J. P. Coon, and M.-A. Badiu, "Chernoff bounds and saddlepoint approximations for the outage probability in intelligent reflecting surface assisted communication systems," *arXiv preprint arXiv:2008.05447*, 2020.

[29] D. Kudathanthirige, D. Gunasinghe, and G. Amarasuriya, "Performance analysis of intelligent reflective surfaces for wireless communication," in *ICC 2020-2020 IEEE International Conference on Communications (ICC)*. IEEE, 2020, pp. 1–6.

[30] T. Wang, G. Chen, J. P. Coon, and M.-A. Badiu, "Study of intelligent reflective surface assisted communications with one-bit phase adjustments," *arXiv preprint arXiv:2008.09770*, Aug 2020.

[31] M.-A. Badiu and J. P. Coon, "Communication through a large reflecting surface with phase errors," *IEEE Wireless Communications Letters*, vol. 9, no. 2, pp. 184–188, 2019.

[32] P. S. Bithas, K. Maliatsos, and A. G. Kanatas, "The bivariate double Rayleigh distribution for multichannel time-varying systems," *IEEE Wireless Communications Letters*, vol. 5, no. 5, pp. 524–527, 2016.

[33] S. Rahman and H. Xu, "A univariate dimension-reduction method for multi-dimensional integration in stochastic mechanics," *Probabilistic Engineering Mechanics*, vol. 19, no. 4, pp. 393–408, 2004.

[34] E. W. Weisstein, *Modified Bessel Function of the Second Kind From MathWorld-A Wolfram Web Resource*, (accessed Januray 6, 2021). [Online]. Available: https://mathworld.wolfram.com/ModifiedBesselFunctionoftheSecondKind.html

[35] ——, *Confluent Hypergeometric Function of the First Kind-A Wolfram Web Resource*, (accessed Januray 6, 2021). [Online]. Available: https://mathworld.wolfram.com/ConfluentHypergeometricFunctionoftheFirstKind.html

[36] Z. Zhang, Y. Cui, F. Yang, and L. Ding, "Analysis and optimization of outage probability in multi-intelligent reflecting surface-assisted systems," *arXiv preprint arXiv:1909.02193*, 2019.

[37] M. Srinivasan and S. Kalyani, "Approximate random matrix models for generalized fading MIMO channels," *arXiv preprint arXiv:1707.09734*, 2017.

[38] E. W. Weisstein, *Digamma Function From MathWorld-A Wolfram Web Resource*, (accessed Januray 6, 2021). [Online]. Available: https://mathworld.wolfram.com/DigammaFunction.html